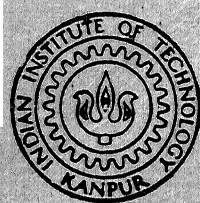


# SLIDING WEAR STUDY OF HEAT TREATED AND CARBURIZED STEEL WITH CLADDINGS

*by*  
DHANANJAY KUMAR

ME  
1989  
M  
KUM



DEPARTMENT OF METALLURGICAL ENGINEERING  
INDIAN INSTITUTE OF TECHNOLOGY KANPUR

DECEMBER, 1989

561A2  
1035S

# **SLIDING WEAR STUDY OF HEAT TREATED AND CARBURIZED STEEL WITH CLADDINGS**

*A Thesis Submitted  
in Partial Fulfilment of the Requirements  
for the Degree of*

**MASTER OF TECHNOLOGY**

588501

*by*  
**DHANANJAY KUMAR**

*to the*  
**DEPARTMENT OF METALLURGICAL ENGINEERING  
INDIAN INSTITUTE OF TECHNOLOGY KANPUR  
DECEMBER, 1989**



- 5 APR 1990

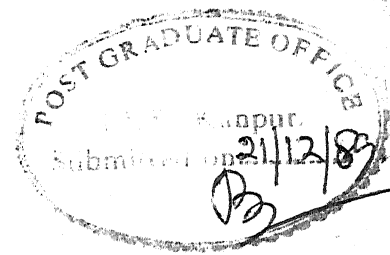
CENTRAL LIBRARY  
I. I. T., KANPUR

107887

No. A

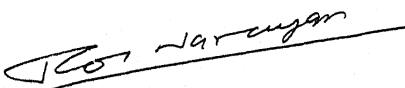
Th  
669.142  
D535S

ME-1989-M-KUM-SLI



## C E R T I F I C A T E

This is to certify that this work "Sliding Wear Study of Heat Treated and carburized steel with Cladings" has been carried out by Mr. Dhananjay Kumar under our supervision, and it has not been submitted elsewhere for a degree.

  
Dr. Raj Narayan  
Professor.

  
Dr. M.L. Vaidya  
Professor

Department of Metallurgical Engineering  
Indian Institute of Technology  
Kanpur, India.

## ACKNOWLEDGEMENTS

I take this opportunity to express my deep sense of gratitude towards Dr. M.L. Vaidya and Dr. Raj Narayan with whom it was great pleasure to work for last one and a half years. Their invaluable guidance could only help me to complete my thesis within stipulated time.

I am grateful to the manager of "Track parts India Ltd." who supplied us the sample and also did necessary heat-treatment for our sample.

I would also like to thank my ever cheerful freinds like Dr. Manisha Tripathi and Mr. M.G. Bhangui who encouraged me at each and every stage and helped me in typing my thesis.

Finally, I would like to thank Mr. M.N. Mungole who helped me in experimental work.

Dhananjay Kumar.

## LISTS OF CONTENTS

CONTENTS	PAGE No.
ABSTRACT	1
1. INTRODUCTION	2-3
2. GENERAL REVIEW OF SLIDING WEAR PHENOMENON	4-22
2.1.1. ADHESION THEORY OF WEAR	4-5
2.1.2. DELAMINATION THEORY OF WEAR	5-7
2.1.3. VOID NUCLEATION	7-8
2.1.4. CRACK PROPAGATION	8
2.1.5. WEAR IN LUBRICATED CONDITION	8-9
2.1.6. CONDITION FOR DELAMINATION	9
2.1.7. EFFECT OF SURFACE ROUGHNESS	9
2.1.8. WEAR MINIMIZATION	9-11
2.1.9. WEAR OF IRON & ITS ALLOY	11-12
2.2. WEAR RESISTENT COATING	13-22
3. EXPERIMENTAL PROCEDURE	23-30
3.1. MATERIAL PROPERTIES & HEAT TREATMENT	23
3.2. SAMPLE SHAPE & SIZE	23
3.3. Cr- COATING & Cr-GRAPHITE COMPOSITE COATING	23-24
3.4. MICROGRAPHS	24
3.5. WEAR-TESTING	25-28
4. RESULTS & DISCUSSION	31-70
4.1. DRAPHS & DISCUSSION	35-65
4.2. MICROSCOPIC OBSERVATION OF THE WEAR SHEET FORMATION BY DELAMINATION	66-70
5. CONCLUSIONS	71
6. SCOPE OF FURTHER STUDIES	72
7. REFERENCES	73

## ABSTRACT

Sliding wear studies under zero lubrication conditions between carburised heat treated low carbon steel and heat treated (quenched and tempered) medium carbon steel have been carried out. The carburised component formed the stationary object over which the heat treated medium carbon steel component was slid in an Amsler machine. Following significant results have been obtained.

- (i) For nearly equal surface hardness conditions, the carburised heat treated component wears off faster than the heat treated medium carbon steel.
- (ii) The initial wear losses are significantly higher than the subsequent periods. Also, the losses are higher for higher loading conditions.
- (iii) If both the components are made out of heat treated medium carbon steels the wear losses are considerably reduced.

Experiments were also carried out to decrease wear losses by coating the carburised heat treated component with chromium and composite chromium-graphite coatings. The results were:

- (iv) Chromium coatings reduce the wear losses in general but significantly at higher loads. However the wear losses of the medium carbon heat treated steel increased against the coated steels.
- (v) Chromium-graphite coatings are better than chromium coatings in controlling the wear losses.

The results have been explained in terms of the existing wear mechanism of sliding wear without lubrication.

## CHAPTER 1

### INTRODUCTION:

With the passage of time, most of the materials in our world wear out. The extent of wear is dependent on the force with which the material comes into contact with other body, nature of interface i.e. lubricated or not, surface roughness, speed of the sliding surfaces and the nature of the material.

It is not only the material loss which matters but also the deterioration of the shape and dimensions of the body concerned. Former factor is tolerable if the loss is not too much but the second factor may become fatal to the further application of the body even if it is small. So, it is to control the second factor that we control the first factor i.e. material loss.

In all pure sliding phenomenon one surface is moving against the other which is kept fixed and in this process a time will come when these two interacting surfaces are not making proper contacts or, from strength point of view this is not at all fit and in this situation there is no way except replacing that particular part or sometime the whole machine has to be abandoned. So, if by some surface treatment like Cr-cladding or Cr-graphite cladding sliding wear is minimized it will certainly improve the life of machine and maintenance cost can be cut down.

In bush-sprocket drive system of tanks and all heavy earth moving earth vehicles at one particular instant one tooth of a sprocket gets engaged with a bush and it pushes forward. In this process interacting face of the tooth of the sprocket slide over the bush surface and this practical case can be compared to a pure sliding process where one surface is moving against a surface which is static. According to one statistical estimation, after almost 5000 working hours bush face gets thin enough that the joining pin which keeps two adjoining bush together gets too much loaded and it breaks very frequently. So in this case there is no choice but to replace that worn out bush.

Cladding of any hard material over the bush is one of the way to control the sliding wearing process. Chromium is supposed to be fairly hard material and its cladding by electrodeposition process is fairly easy.

All earth moving vehicles and tanks have to work in extreme climatic condition full of dust and mud and so in such cases liquid lubrication is inefficient. So, if solid lubrication is used in cladding process as a composite then it will certainly improve the working life of bush material. Graphite is the most common solid lubricant which is codeposited with chromium as a composite.

The present study deals with sliding wear mechanism study of carburized and heat treated steel used for bush and sprocket material respectively. Later on Cr-coating on carburized sample is

carried out and then again sliding wearing study was performed. After that sliding wear mechanism study of heat treated sample was performed with both sample made of the same material.

In the end Cr-graphite composite coating was performed, where graphite acts as a solid lubricant and then once again sliding wear study was performed.

## CHAPTER 2

### GENERAL REVIEW OF SLIDING WEAR PHENOMENON

Wear is a widely known phenomenon and it is one of the most important cause of the failure of machine parts. When ever two surfaces interacting there are number of forces like frictional force, viscous force, electromotive force acts ~~at it which acts~~ on the surface material. In this process surface or subsurface material either comes out in a continuum or in form of chips or in any other forms like flakes etc. Thus in all wear process surface material get eroded and hence there is net loss of surface material.

Sliding wear is one form of wear when one surface is stationary and other surface is performing pure skidding on it. It is a idealised case where there is only translational movement of one surface against other which is stationary. This is a pure translational motion without any rotational segment.

For our experimental purpose we used two ring type sample one of which is rigidly clamped and another one which is rotating with pure sliding at the stationary sample surface. Here if the surface in contact is only studied then one surface is moving tangentially against the other without rotation, though one sample is rotating in pure sense. Thus, it is also a pure sliding case.

Sliding wear is dependent on various factors like hardness of the material, the coefficient of friction, microstructure of the material and the surface roughness.

#### 2.1.1 ADHESION THEORY OF WEAR:

It states that wear mainly takes place at the surface and in this process material loss takes place mainly from the surface and not from inside. Thus according to this theory surface properties like friction coefficient, surface hardness, surface roughness etc. will play major role and inside microstructural study is irrelevant for wear study.

But later wear-study showed that adhesion mode of wear is just insignificant part and it is insufficient to explain many of the wear experiment results. Later on it was found that harder surface even wear faster than softer surface which contradicts the adhesion theory of wear mechanism.

So after extensive detailed study more relevant theory of



wear mechanism was propounded which was called "Delamination Theory of Wear"

### 2.1.2 MECHANISM OF DELAMINATION WEAR

#### General Description,

The delamination (33,34) theory of wear describes the following sequential (or independent, if there are preexisting sub-surface cracks) events which leads to wear particle formation.

- (a) When two sliding surfaces come into contact, normal and tangential loads are transmitted through the contact points by adhesive and ploughing actions. Asperities of softer surface are easily deformed and some are fractured by the repeated loading actions. A relatively smooth surface is generated either when these asperities are deformed or when they are removed. Once the surface becomes smooth, the contact is not just asperity to asperity contact, each point along the softer surface experiences a cyclic loading as the asperities of the harder surface plough it.
- (b) The surface traction exerted by the harder asperities on the softer surface induces plastic shear deformation which accumulates with repeated loading.
- (c) As the sub surface deformation continues, cracks are nucleated below the surface. Crack nucleation very near to the surface is not favoured because of a triaxial state of highly compressive stress which exists just below the contact regions.
- (d) Once cracks are present (owing either to the crack nucleation process or to pre-existing voids), further loading and deformation causes extension and propagation, joining neighbouring ones. The cracks tend to propagate parallel to the surface at a depth governed by materials properties and the coefficient of friction. When cracks cannot propagate because of either deformation or an extremely small tangential traction at the asperity contact, crack nucleation is the rate controlling mechanism.
- (e) When these cracks finally shear to the surface (at certain weak positions) long and thin wear sheets delaminate. The thickness of a wear sheet is controlled by the location of sub surface crack growth, which is controlled by the normal and the tangential loads at the surface.

Also some metal oxides are reported to be formed on the wear surface depending upon the temperature of the experiment or the heat generated during wear or combined effects of above two.

Glazes are formed when oxide particles are embedded in the metal surface matrix due to the force acting and also the wear action. This metal-cum-oxide layer reduces the friction generally in turn reducing wear.

The development of glaze probably involves three simultaneous stages (42); formation agglomeration and compaction of oxide debris. Following oxide debris a relatively weak bond which causes the debris particles to adhere, is developed. Compaction of the particles under pressure between the sliding surfaces increases this bonding by increasing number of contact points between the particles and enlarging the existing areas of contact. The external pressure promotes closer packing of the particles by a process of redistribution and deformation. As the applied pressure increases; the strength of the compact increases. The compaction of oxide powders is a long established process used to fabricate ceramic components, known as hot pressing.

It is apparent that the the very smooth nature of the glaze surface is due to continuation of oxide to give very fine particles plastic flow of the oxide. During sliding, interaction between contacting asperities result in development of junctions. If asperities are mettalic these junctions can grow significantly, resulting in relatively high coefficients of friction while subsequent wear can be substantial.

However with oxide asperities the junctions grow relatively little before failure occurs. The termination of junction growth occurs when the contact area has increased to such an extent that the reduced pressure over the points of contact results in the oxide reverting to its brittle nature ie when the hydrostatic pressure and the Auerback effect no longer operate. Thus under high contact pressure, small cracks, which cause a reduction in the effective shear strength of oxide are partially heated up, as junction growth proceeds; and the contact pressure is reduced. Such cracks enlargement act more effectively as stress rises, leading to a reduction in shear strength of oxide and ultimately to brittle failure of the junctions. Hence the coefficient of friction is significant but considerably lower than that recorded when metal-metal junctions are able to form. Wear rate is low because the oxide wear debris produced consists of very fine particles which are either recompacted into the glaze surfaces from which they originated or are transferred and compacted into the opposing glaze surfaces.

## THEORY

The proposed delamination theory of wear is based on the following reasoning.

(a) During wear the material at and very near the surface does not have a high dislocation density, due to the elimination of dislocations which are parallel to the surface. Therefore, the material very near the surface cold-worked less than that of the subsurface layer.

(b) With continued sliding there will be pile-ups of dislocations at a finite distance from the surface. In time this will lead to the formation of voids. The formation of voids will be enhanced if the material contains a hard second phase to dislocations to pile against. Voids form primarily by plastic flow of matrix around hard particles, when there are large secondary phase particles in the metal.

(c) With time the voids will coalesce, either by growth or shearing of the metal. The end result is a crack parallel to the near surface.

(d) When this crack reaches a critical length (dependent upon the material), the material between the crack and the surface will shear, yielding a sheet like particle.

(e) The final observed shape of the particle will be dependent upon its length and internal strains.

### 2.1.3 VOID NUCLEATION

The process of void nucleation around rigid inclusions of circular cross section embedded in an elastic plastic matrix in plane strain subjected to pure shear and superposed hydrostatic tension is given by the equation (43)

where

$$\sigma_{rr} = y(\epsilon^{-p}) + \sigma_h$$

$\sigma_{rr}$  = maximum interfacial stress

$y(\epsilon)$  = yield strength of the material

$\sigma_h$  = hydrostatic stress

Void nucleation is then possible if  $\sigma_{rr}$  reaches the particle matrix bond strength.

The equation is modified to

$$(\sigma_{rr}) = \sqrt{3} K \sin 2\theta_0 + 3 \tau_{\max} \sin 2(\theta_0 - \theta) + \sigma_h$$

$\tau_{\max}$  = maximum shear stress at the point (x,y).

$\theta$  = angle from x axis to the axis of the maximum positive shear stress.

$\sigma_h$  = Hydrostatic stress at (x,y).

$\theta_0$  = the angle at which  $(\sigma_{rr})$  occurs.

The voids, which cannot form at the surface due to the large hydrostatic pressure which exists directly under the contact, can

nucleate below a depth where the hydrostatic pressure is not large enough to suppress void formation and above a depth where the plastic deformation is insufficient to nucleate voids around the hard particles. The size and the depth of this region increases with increasing friction coefficient and normal load. The number of passes required for void nucleation at a given depth decreases with increasing friction coefficient.

#### 2.1.4 CRACK PROPAGATION:

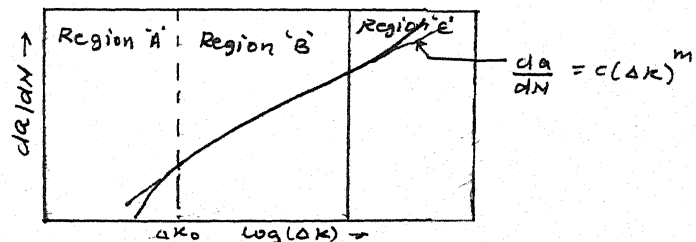
The mechanism of crack propagation is not known correctly. It is assumed to follow fatigue crack growth rate (36) and some of the other aspects are discussed in (35).

If the crack extension per loading cycle  $da/dN$  is plotted against the logarithm of the change in stress intensity factor  $\Delta K$  at the tip of the crack, the shape of the curve is independent of the material. A typical curve is shown in Fig.

A region = Threshold regime

B region = A steady growth regime

C region = Static mode regime.



In the threshold regime the average crack extension per cycle is of the order of atomic dimension or less. Thus continuum mechanics does not apply in this region and the crack grows in spurts. In the static mode regime the crack extension per cycle is on the order of particle size. continuum mechanics applies but, since the stress intensity factor at the tip of a crack increases significantly in each cycle owing to the large extension, the relationship between the crack extension and the logarithm of the stress intensity factor is non-linear.

In the steady growth regime cracks grow at a constant extension per cycle and the stress intensity factor increases slowly. Fatigue striations are produced. It has been shown empirically that the relationship between  $\Delta K$  and  $da/dN$  in the steady growth regime is of the form

$$da/dN = C (\Delta K)^m$$

where  $C$  and  $m$  are material properties,  $m$  is usually of the order 3 to 4.

#### 2.1.5 WEAR IN LUBRICATED CONDITION

The process of wear particle formation under lubricated sliding conditions is greatly affected by the tangential stresses (40). The tangential force can be varied, keeping the normal load constant, by the addition of friction affecting material in the lubricating oil. The wear rate at the level of surface are greatly reduced if the friction coefficient is lower than a specific threshold value. Under these conditions

wear particles are formed from deformation of surface asperities. At higher friction coefficient more wear occurs by the process of plowing and delamination under severe wear condition and lubrication failure, extremely large amounts of wear and severe surface result from adhesive wear mechanism.

#### 2.1.6 CONDITION FOR DELAMINATION:

If  $\mu$ , friction coefficient defined when plateaux are firmly attached to the base material, is greater than  $\mu_c$ , friction coefficient when sliding occurs between the plateaux and the base material, then wear occurs by delamination. This occurs when plateaux exceed a critical thickness (37).

#### 2.1.7 EFFECT OF SURFACE ROUGHNESS:

The initial wear rate is influenced by the surface roughness and the applied load but at steady state wear rate is independent of the initial roughness (38). Under low applied loads delamination of smooth surfaces commence soon after sliding is initiated, where as delamination of rough surface is delayed until the original asperities are worn. Consequently under low loads, the initial wear rate of a smooth surface is higher than that of a rougher surface. The opposite is found to occur under high loads since original asperities are removed immediately. If any machining damage is left on the specimen surface or sub-surface (in the form of deformation, voids and cracks) it will accelerate the initial wear rate of machined surface.

#### 2.1.8 WEAR MINIMIZATION:

The factors responsible for wear or the wear is affected mainly by (a) Surface tractions (b) microstructure of the material and (c) quality of the surface and (d) coatings. By controlling the above factors, the wear can be minimized. (39).

##### (a) Surface Traction:

The wear rate is significantly affected by the magnitude of the normal and the tangential loads. The normal load is controlled by the external conditions and basic nature of the magnitude of the tangential load. By the addition of lubricants to the interface the tangential load can be controlled. (40).

The coefficient of friction is affected by the adhesion and plowing (41). The plowing component of the frictional force decreases as the hardness is increased by such techniques as solid solution hardening, which in turn decreases the wear rate significantly. Therefore, it is highly desirable to make the surface as hard as possible without introducing crack nucleation sites.

An identical or similar pair of metals has a greater tendency for adhesion than those which differ to the extent of not forming solid solutions. So it is better to select metals which do not form solid solutions.



Since the crystallographic orientation of metals near the surface changes so that the slip planes line up parallel to the surface, the frictional force is lowered by the easier slip (especially in the absence of plowing). The hexagonal closepacked (h. c. p.) metals having higher  $c/a$  ratio are recognised as metals with easy slip. One technique of making use of slip properties of such h. c. p. metals is to disperse a small volume fraction of hard particles such as WC in an h. c. p. matrix such as Co. (They form a solid solution). In such system, the normal load is carried by the hard particles and the matrix provides low friction properties.

#### (b) MICROSTRUCTURE OF THE MATERIAL:

The raise in hardness reduces the subsurface void formation and the raise in toughness decreases the crack propagation. But it is not possible to raise both using a manipulation leading to a single micro structure. So the micro structure can be optimized to give reasonably higher values of both.

Carburizing and nitriding are certainly desirable to reduce wear.

The II phase particles reduce the wear but they become easier site for nucleation if the size is more than 200  $\text{\AA}$ .

By fibre reinforcement perpendicular to the surface of wear, the wear can be controlled, because the crack propagation (parallel to the surface) is hindered. But the parallel reinforcement is not desirable. The friction coefficient is higher and wear is minimum in the former case.

#### (c) Surface Quality

As discussed already, the surface finish should not have any damage due to machining.

Since the tangential component of the surface traction can increase to a large value when there is a long range variation of the surface profile (ie. waviness), the wear rate can be increased significantly owing to the waviness. So the waviness of the surface should be avoided.

#### (d) Coating Techniques:

Notwithstanding the controversy concerning the dynamics of dislocations near a surface layer bonded to a hard substrate can reduce the wear rate by several orders of magnitude. In general, the thickness of the soft layer must be of the order of 0.1  $\mu$ . Such a coating is effective even at high speeds and prevents seizure even in situations when seizure would occur immediately upon contact in the absence of coating.

Hard coatings can be better than softer coating (ie it

opposes abrasive wear also ) and it should be of depth of minimum 200 nm which is the maximum limit for plastic deformation during sliding. The coating should be coherent.  $Al_2O_3$ , WC, TiC and HfC can be coated on metal by chemical vapour deposition (CVD) method.

Laser heating may help in producing super-saturated solid solution on the surface by rapid heating and cooling.

Some oxide produced during sliding may be smooth and may form a coating like layer on the surface. This is desirable to have which will reduce wear, but at the same time it should not be removed quickly.

#### 2.1.9 WEAR OF IRON AND ITS ALLOY:

The iron and its alloys, widely used materials, also subjected to wear tests. A simple model, based on linear oxidation, was proposed to represent oxidative wear by flaking.

The theory developed predicted that  $\log(N/w)$  varies with  $O$  where  $N$  is the normal applied force,  $w$  = wear rate per time and  $O$  = the absolute temperature of the metal substrate. The results of tests using En1A pins on N 75 and En1A tracks showed reasonable agreement with the theoretical predictions for  $O$  values between 300 C and 500 C for both the N75 track and En1A track (11). In these regions oxidation might reasonably be expected to constitute the majority of the wear.

The results were used to estimate values for the activation energies which were of the right order of magnitude bearing in mind the likely variations in the oxidation rate between running and static conditions. Comparison of activation energies for En1A/N75 and En1A tests appeared to indicate that abrasion by the track is likely to be important when considering wear. The theory was developed to apply to parabolic oxidation.

The alloys Fe-Cr (5-20% Cr) were studied in unidirectional and reciprocating motions (12) under conditions where frictional heating should be minimal. These experiments were performed in an ultrahigh vacuum chamber in which the oxygen partial pressure could be maintained from  $10^{-6}$  Pa to atmospheric pressure. At  $10^{-6}$  Pa the friction behaviour and the pattern of wear were essentially similar for both types of motion, although slightly lower wear was observed under reciprocating motion. At higher oxygen partial pressures the containment of debris within the track led to the formation of compacted oxide 'islands'. Hemispherical upper specimens seemed more effective than the conical cones in trapping this debris. The islands developed gradually but increasingly rapidly as the oxygen partial pressure was increased (13) which could persist for extended periods during subsequent evacuation.

Evidence from various experimental techniques indicated that the compacted debris was a mixture of alloy and oxides in the

form of oxide covered particles.

Friction experiments of Fe and Fe-Cr (0.40%) in the temperature range of 20-850 C in the pressure of 10 Pa were conducted (45). High temperature micro hardness tests made on the materials showed that hardness and coefficient of friction values were not closely related, but that the coefficient of friction might be correlated with the ductility of the metal. The only alloy not to exhibit seizure during sliding in 10 Pa at high temperature was Fe-40% Cr.

The effect of sliding speed as wear and friction was studied (15) by Saka on AISI 1020 steel AISI 304 stainless steel and commercially pure Ti (TSA) using pin on ring geometry, in air, without any lubricant. The sliding speed was 0.5 - 10 m.sec and the normal force was 49 N (5 kgf). It was found that the friction coefficient decreased with sliding speed. This appeared to be a consequence of oxide formation. The wear rate of 304 stainless steel increased monotonically with speed, whereas the wear rate of 1020 steel and Ti first decreased and then increased and again decreased with a maximum occurring at about 5 m. sec. The complex variation of wear rate as a function of speed is explained in terms of the dependence of the friction coefficient, hardness and toughness of the materials on temperature.

Microscopic examinations of the wear track, the subsurface of worn specimens and the wear particles indicated that the wear mode was predominantly by subsurface deformation, crack nucleation and growth processes, ie delamination process, similar to the low speed sliding wear of metals: oxidative and adhesive theories proposed in the past to explain the high speed sliding wear of metals were found to be incompatible with the experimental observations.

Using a rotating beam test the combined wear-fatigue life of medium carbon steel (SISI-1045) was investigated under various combinations of loads. The direction of maximum tensile stress due to bending was perpendicular to that due to wear. Tests were also performed with specimens plated with a thin layer of cadmium or Ni-Au. All of the tests were conducted in the high cycle regime. The results showed that the fatigue life of all the specimens at a stress level higher than the endurance limit of the specimen was within the experimental scatter of typical fatigue test. The effect of sliding imposed by the slider on fatigue life was manifested primarily by the stress field imposed by the slider on the specimen. In the case of plated specimens the fatigue life was not significantly affected, although the wear rate was decreased by an order of magnitude.



## 2.2 WEAR RESISTANT COATING

### 2.2.1 INTRODUCTION

Electrodeposited composites are produced by suspending the second phase material, in the form of fine powder or filament, in a conventional plating electrolyte. These particles are held in suspension throughout the plating period by agitation. Different forms of agitation have been employed such as mechanical stirring, air or gas bubbling, electrolyte recirculation, ultrasonic agitation and plate pumping.

Depending upon the intended application composite coatings could be categorized into following:

- 1.) Wear resistant coatings.
- 2.) Dry lubricant coatings.
- 3.) Heat-treatable metal alloy coatings.
- 4.) Nuclear control coatings.

### 1.WEAR RESISTANT COATINGS:

Many investigators believed that the wear resistance of composite coatings was largely governed by the wear properties of the hard particles, provided the wear load was less than the compression yield strength of the matrix material. They thought that when a composite coating having hard particles dispersed in it is brought into contact with a sliding counterface the wear continues till the hard particles are exposed so that they bear the wearload. Based on these assumptions attempts have been made to disperse various hard particles like Al<sub>2</sub>O<sub>3</sub>, TiO<sub>2</sub>, SiC, WC, Cr<sub>2</sub>O<sub>3</sub>, TiC, diamond, etc. Table 1.1 gives physical

properties of some materials which affect the wear behaviour of

composite coatings. Kedward, however, pointed out that in actual practice a certain amount of metal to metal contact was inevitable due to the non-uniformity of the applied load over the wearing surface. Thus for good wear properties, they pointed out, it is essential to recognise the importance of both the particles dispersed and the matrix metal. Maximum wear resistance, according to them, would be obtained when hard particles are dispersed in a hard and wear resistant matrix. Based on these arguments they developed composite Co-alloy coatings. These coatings had better wear resistance than all other coatings developed by them. However, more work is needed to confirm their conclusions.

### 1.a CHROMIUM BASED WEAR RESISTANT COATINGS:

Chromium is attractive as a matrix metal in a number of ways, although primarily for its good wear and oxidation properties. Various baths have been tried for composites coatings (Table 1.3).

## 1.b CHROMIUM-REFRACTORY OXIDES:

Early attempts to codeposit  $\text{Al}_2\text{O}_3$  and  $\text{SiO}_2$  with chromium, baths from hexavalent and trivalent baths proved (5,6) unsuccessful. However, Skominas et al reported that the codeposition of  $\text{Al}_2\text{O}_3$ ,  $\text{SiO}_2$ ,  $\text{ZrO}_2$  with chromium was possible from an hexavalent bath. They concluded that  $\text{Al}_2\text{O}_3$  of particle size 1-2 microns was well suited for composite coating. With increase in alumina content in the bath and decrease in current density the codeposition of  $\text{Al}_2\text{O}_3$  increased. A similar behaviour was observed in case of  $\text{SiO}_2$  also.

(8)  
Addison and Kedward investigated both hexavalent electrolytic systems for codepositing  $\text{Al}_2\text{O}_3$ . It was observed that hexavalent bath was not suitable for composite coatings whereas codeposition could be achieved with trivalent baths. However, there was a severe limitation on the thickness of coating obtainable from trivalent baths, which may prove to be a drawback in wear problems. Moreover, uniform coating thickness could not be obtained from trivalent chromium bath based on chlorides (6) because of its poor throwing power. Young also has shown that  $\text{Al}_2\text{O}_3$  could not be codeposited from hexavalent baths. He also

+  
showed that the presence of Tl (Thallium ion) in the bath made codeposition possible.

Wear properties of  $\text{Cr-Al}_2\text{O}_3$  composite coatings, (8) (6)  
produced both from trivalent and hexavalent baths, were reported to be inferior to those of hard chromium coatings. (6)  
Young observed that average wear loss was more of  $\text{Cr-Al}_2\text{O}_3$  composites than that of chromium (Table 2.4). Addison and (8)  
Kedward reported that upto a temperature of about 200 °C the wear resistance of  $\text{Cr-Al}_2\text{O}_3$  composite coating is higher than that of pure chromium coating. At temperatures above 200 °C the wear resistance of composite coatings was much inferior to that of chromium coating (Fig 2.1).

### 1.b CHROMIUM-REFRACTORY OXIDES:

Early attempts to codeposit  $\text{Al}_2\text{O}_3$  and  $\text{SiO}_2$  with chromium, baths from hexavalent and trivalent baths proved (5,6) unsuccessful. However, Skominas et al reported that the codeposition of  $\text{Al}_2\text{O}_3$ ,  $\text{SiO}_2$ ,  $\text{ZrO}_2$  with chromium was possible from an hexavalent bath. They concluded that  $\text{Al}_2\text{O}_3$  of particle size 1-2 microns was well suited for composite coating. With increase in alumina content in the bath and decrease in current density the codeposition of  $\text{Al}_2\text{O}_3$  increased. A similar behaviour was observed in case of  $\text{SiO}_2$  also.

(8)  
Addison and Kedward investigated both hexavalent electrolytic systems for codepositing  $\text{Al}_2\text{O}_3$ . It was observed that hexavalent bath was not suitable for composite coatings whereas codeposition could be achieved with trivalent baths. However, there was a severe limitation on the thickness of coating obtainable from trivalent baths, which may prove to be a drawback in wear problems. Moreover, uniform coating thickness could not be obtained from trivalent chromium bath based on chlorides (6) because of its poor throwing power. Young also has shown that  $\text{Al}_2\text{O}_3$  could not be codeposited from hexavalent baths. He also

+  
showed that the presence of Tl (Thallium ion) in the bath made codeposition possible.

Wear properties of  $\text{Cr-Al}_2\text{O}_3$  composite coatings, (6)  
produced both from trivalent and hexavalent baths, were reported to be inferior to those of hard chromium coatings. (6)

Young observed that average wear loss was more of  $\text{Cr-Al}_2\text{O}_3$  composites than that of chromium (Table 2.4). Addison and (8) Kedward reported that upto a temperature of about 200°C the wear resistance of  $\text{Cr-Al}_2\text{O}_3$  composite coating is higher than that

of pure chromium coating. At temperatures above 200°C the wear resistance of composite coatings was much inferior to that of chromium coating (Fig 2.1).

2

Greco and Baldauf<sup>2</sup> successfully codeposited TiO<sub>2</sub> with chromium from hexavalent bath. The volume per cent of TiO<sub>2</sub> in chromium was 1.0% compared to approximately 13 V/O of TiO<sub>2</sub> in nickel for same bath concentrations and current density. Hardness measurements for 1.0 v/o TiO<sub>2</sub> in chromium gave results between 1550-2300 compared to 900-100 for pure chromium on the Knoop scale.

### 1.c CHROMIUM-REFRACTORY CARBIDES, BORIDES AND DIAMOND:

Various refractory carbide and boride particles codeposited with chromium include SiC<sup>(6,10,11)</sup>, B<sub>4</sub>C<sup>(6,10)</sup>, B<sub>6</sub>C<sup>(6,10)</sup>, TiC<sup>(26)</sup>, Cr<sub>3</sub>C<sup>(6)</sup>, ZrB<sub>2</sub><sup>(9,12)</sup> and TiB<sub>2</sub><sup>(6)</sup>. Diamond particles have also been successfully codeposited with chromium<sup>(6)</sup>.

Young<sup>(6)</sup> observed that codeposition of various carbides such as SiC<sub>4</sub>, B<sub>4</sub>C<sub>6</sub>, B<sub>6</sub>C and TiC with chromium from the conventional hexavalent bath was not possible without the addition of monovalent ions like Tl<sup>+</sup>, Ce<sup>+</sup>, Li<sup>+</sup>, NH<sub>4</sub><sup>+</sup> and Na<sup>+</sup>. Of these Tl<sup>+</sup> ion was most effective with all the carbides mentioned except with SiC where Ce<sup>+</sup> ion gave better codeposition than Tl<sup>+</sup> ions. At high concentrations Li<sup>+</sup>, Na<sup>+</sup> and NH<sub>4</sub><sup>+</sup> ions caused deleterious effect on the properties of chromium deposit. However, when used in small quantities they were effective in bringing about the codeposition of particles.

+

With increase in Tl<sup>+</sup> ion concentration, the amount of SiC codeposited with chromium increased in the conventional hexavalent bath and decreased in Bernhauser bath<sup>(6)</sup>.

+

Codeposition of B<sub>4</sub>C was not very sensitive to operating variables like Tl<sup>+</sup> ion concentration, temperature, and current

(8)  
Addison and Kedward codeposited  $\text{Cr}_3\text{C}_2$  particles with chromium from trivalent bath. But the wear resistance of composite coating was much inferior to hard chromium coatings over a temperature range of 0-400 C (Fig.2.1).

Wear resistance of various composite chromium coatings has been reported by Young (6). It was observed that next to diamond, inclusion of  $\text{B}_6\text{C}$  was most effective in increasing the wear resistance of chromium coating (Table 2.3)

Composite  $\text{Cr-ZrB}_2$  coatings exhibited good wear characteristics between 300-400 C and after 400 C the wear resistance decreased (Fig.2.1).

(31)  
Kedward et al claimed that preworking of the conventional hexavalent bath with dummy cathodes and then plating on to the required substrate produced  $\text{Cr-ZrB}_2$  composite coatings with evenly dispersed  $\text{ZrB}_2$  in chromium.

Codeposition of diamond particles with chromium from hexavalent bath containing additions of  $\text{Tl}^+$  ions has been reported by Young (6). When diamond was coated with nickel (electrolessly) then the amount of codeposition increased. With an increase in  $\text{Tl}^+$  ion concentration in the bath the amount of diamond in the composite coating increased linearly (26). The amount of diamond in the composite coating decreased with increase in current density and the effect was more pronounced in conventional hexavalent bath than in Bornhauser bath. Wear resistance of these Cr-diamond composite were reported to be very good (Table 2.3).

## 2 DRY LUBRICANT COATINGS:

Instead of hard particles, if soft particles having low shear strength are dispersed in metal matrix then the resulting composite coating may be expected to possess good antifriction properties. Various particles codeposited with metal to produce dry lubricant composite coatings include molybdenum disulphide, graphite and barium sulphate.

Ni-MoS<sub>2</sub> composites have been reported by various investigators (13-17) (13) Vest an Bazarre codeposited MoS<sub>2</sub> with nickel from sulphamate bath. pH was found to have a pronounced effect on the codeposition. Increase in pH decreased the volume percent inclusion of MoS<sub>2</sub>. The adhesion of the coatings decreased (13,15,17) with inclusion of MoS<sub>2</sub> particles. The internal stress in the composite coating was less than that in nickel coatings. The coefficient of friction of the composite coating was between (13) 0.05-0.18

(6) Young described the codeposition of MoS<sub>2</sub> with chromium. Deposits from bath containing MoS<sub>2</sub> were very poor and after two or three runs the bath became incapable of producing continuous chromium deposits.

(44) Konzina and Erganov codeposited MoS<sub>2</sub> with copper, silver and tin. They observed that coefficient of friction of silver coatings was somewhat reduced when MoS<sub>2</sub> particles were included in it. Inclusion of MoS<sub>2</sub> particles had practically no effect on the coefficient of friction of copper coatings whereas it was slightly increased in case of tin coatings.

(18) Without the use of promoter Zintsova et al were able to codeposit MoS<sub>2</sub> with silver only from sulphate baths and + presence of Tl<sup>+</sup> ions as promoter was necessary when cyanide and cyanoferate baths were used.

Electrolytic conditions were developed by Saifullin et al (19) for nickel-graphite composite coatings could be used for abrasion resistance. Kedward (21) claimed to have codeposited (22) graphite fibres with nickel from sulphamate bath. Loeffler has also described the production of nickel-graphite coatings.

(6) Young was able to codeposit graphite particles with chromium from conventional hexavalent bath only in the presence of  $Li^+$  ions.

Graphite was codeposited, by Saifullin et al (19) with silver from iodide bath.

(23) Tomaszewski et al reported that graphite could codeposit with copper from acid bath even without addition of any promoters like Tl, Rb, etc.

Cu-barium sulphate composite coatings were successfully produced (23) from acid bath only in the presence of promoters such as heavy monovalent ions Tl, Ce, Rb and amines and amino acids. pH was shown to have no significant effect on the codeposition of  $BaSO_4$  particles whereas increase in temperature

decreased the codeposition and the rate of fall was sharp if Tl was used as promoter whereas it was not so sharp if amine promoters were used (23).

It was suggested that these Cu- $BaSO_4$  composite coatings can be used for sliding contacts because of the antistick properties of  $BaSO_4$  particles.



TABLE 2-1 PHYSICAL PROPERTIES OF MATERIALS WHICH AFFECT  
THE WEAR BEHAVIOUR OF COMPOSITE COATINGS

Material	Structure	Density	Melting point ( $^{\circ}\text{C}$ )	Hardness ( $\text{kg/mm}^2$ )
$\alpha\text{-Al}_2\text{O}_3$	Trigonal	3.98	2000	3000
$\gamma\text{-Al}_2\text{O}_3$	Cubic	3.20	2000	
MgO	Cubic	3.58	2850	500
ZrO <sub>2</sub>	Cubic	5.70	2700	1150
SiO <sub>2</sub>	Hexagonal	2.20	1710	
TiO <sub>2</sub> (Rutile)	Tetragonal		1830	
TiO <sub>2</sub> (Anatase)	Elongated Tetragonal			
SiC	Hexagonal	3.20	2700	2500
B <sub>6</sub> C				3000
B <sub>4</sub> C	Rhombohedral	2.52	2350	2800
Cr <sub>3</sub> C <sub>2</sub>	Orthorhombic	6.68	1895	1300
TiC	Cubic	5.48	2730	2500
Wc	Hexagonal		Decomposes before melting	2400
Ni	Cubic	8.19	1455	210
Cr	Cubic, hexagonal	7.14	1893	590
Co	Hexagonal	8.70	1495	125
Cu	Cubic	8.43	1083	80
Au	Cubic	19.30	1063	58



TABLE 2.2 WEAR RESISTANCE OF SOME COMPOSITE CHROMIUM  
COATINGS (Ref. 26)

Particle included in the coating	Coating Properties		
	Hardness (KIN)	Average Wear Loss (mg)	Average Inclusion wt
None	590	9.0	-
$\text{Al}_2\text{O}_3$	602	15.3	1.81
Diamond	662	5.7	0.48
$\text{B}_6\text{C}$	695	6.3	0.30
$\text{B}_4\text{C}$	669	7.5	0.27
$\text{AlB}_{12}$	675	7.7	0.18
$\text{TiB}_2$	662	7.8	0.59
$\text{SiC}$	749	10.2	0.85
$\text{CrB}_2$	607	11.2	0.61
$\text{TiC}$	640	12.2	0.83
$\beta\text{-Si}_3\text{N}_4$	677	12.9	0.33

TABLE 2.3. COMPOSITIONS OF CHROMIUM PLATING BATHSHexavalent Bath

(i)	$\text{CrO}_3$ . . . . .	250 g/l
	$\text{H}_2\text{SO}_4$ . . . . .	2.5 "

## (ii) Bornhauser Bath

	$\text{CrO}_3$ . . . . .	400 g/l
	$\text{H}_2\text{SO}_4$ . . . . .	0.8 "
	$\text{NaOH}$ . . . . .	58 "

Trivalent Baths

(i)	$\text{Cr}_2(\text{SO}_4)_3$ . . . . .	0.5 mole/l
	$(\text{NH}_4)_2\text{SO}_4$ . . . . .	Saturated
	Urea . . . . .	4 mole/l

(ii)	$\text{Cr}_2(\text{SO}_4)_3$ . . . . .	178 g/l
	$(\text{NH}_4)_2\text{SO}_4$ . . . . .	50 "
	$\text{H}_3\text{BO}_3$ . . . . .	2 "
	$\text{Na}_2\text{SO}_4$ . . . . .	50 "
	$\text{HCON}(\text{CH}_3)_2$ . . . . .	100 ml/l (10 v/o)

(iii)	$\text{CrCl}_3$ . . . . .	270 g/l
	$\text{NH}_4\text{Cl}$ . . . . .	10 "
	$\text{NaCl}$ . . . . .	50 "
	$\text{H}_3\text{BO}_3$ . . . . .	2 "
	$\text{HCON}(\text{CH}_3)_2$ . . . . .	420 "

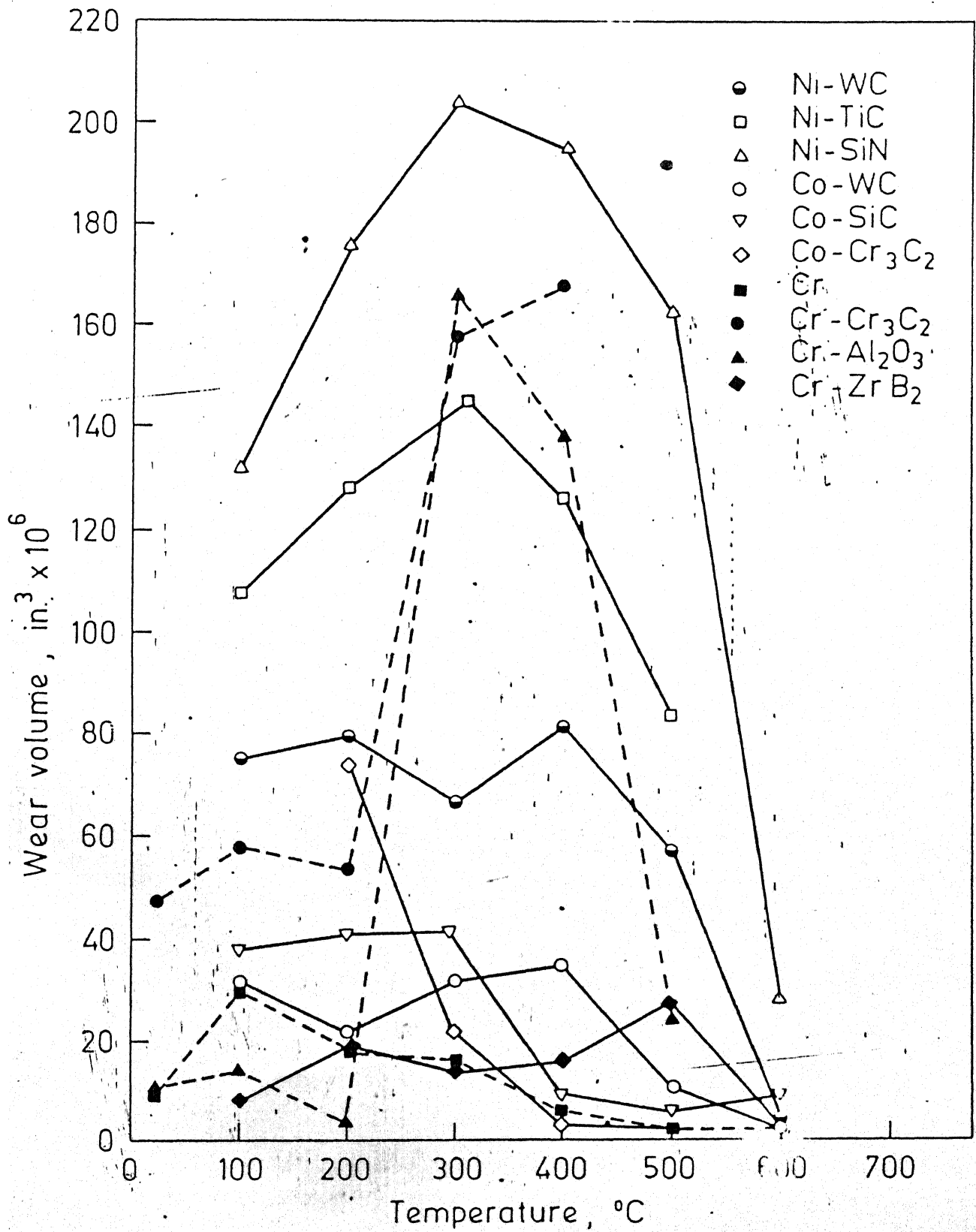


Fig. 2-1 - Wear resistance of various composite coatings (Ref. 17, 28)

## CHAPTER 3

### EXPERIMENTAL PROCEDURE

#### (3.1) MATERIAL PREPARATION & HEAT TREATMENT:

Sprocket material is Boron steel having carbon 0.35%, Boron 0.0002%, Manganese 0.9%. It is water quenched and then tempered at 200°C. ~~It is carburized with a case depth upto 2.5 mm.~~ Its surface hardness is approximately 50 R<sub>c</sub>.

Bush material is manganese, steel with carbon 0.18%, manganese 1%, chromium 0.4%. It is also water quenched and then tempered at 150°C. ~~It is carburized with a case depth upto 2.5 mm.~~ Its surface hardness is approximately 60 R<sub>c</sub>.

#### (3.2) SAMPLE SHAPE & SIZE:

Both sample are taken in a standard cylindrical form as shown in the figures. Both samples are through and through hardened.

#### (3.3) CHROMIUM COATINGS AND CHROMIUM-GRAPHITE COMPOSITE COATINGS:

##### **MATERIALS:**

Following materials were used

- (1) Chromic acid ( $\text{CrO}_3$ ); 99.99% pure, L.R. Grade, S.D's Lab. Chemical Industry, Bombay
- (2) Sulphuric acid, ( $\text{H}_2\text{SO}_4$ ), Sp.gr 1.84, L.R. grade, Sarabhai M. Chemicals Ltd. Wadi-Wadi, Baroda.
- (3) Anode of lead and 8% tin alloy.
- (4) Graphite powder. Average particle size 3-5 $\mu$

##### **EQUIPMENTS:**

- (1) Regulated D.C. power supply. Lambda (LE 104 FM 506).
  - (2) Constant temperature water bath, with a recirculating pump.
- Water was heated, using an immersion heater, in a glass beaker. The electrical power to the heater was supplied through an on/off relay control, A temperature controller, shown in Fig 3.1 was also immersed in the water and the two leads shown in the figure were connected to the on/off relay control. By screwing or unscrewing the brass thread of the temperature controller the temperature of the bath was varied as required. The whole assembly

24

was kept within a metallic casing filled with insulating material like asbestos powder to minimise thermal losses. The top was also covered with an asbestos sheet.

A water circulating pump was used to recirculate the hot water through the double walled glass vat in which the plating experiments were conducted. (Fig. 3.2).

(3.) Speed controlled mechanical stirrer.

(4.) Corning double wall glass vat for the electroplating solution.

#### **ELECTROPLATING SOLUTION:**

The composition of the electroplating bath for chromium is given in table 3.1. The composition corresponds to the conventional chromic acid bath. In experiments where the effect of the variation in composition of the bath was studied, the ratio of sulphuric acid to chromic acid was still maintained at 1:100.

#### **SPECIMEN PREPARATION:**

Carburized steel used for bush material is chosen in standard ring form for both Cr coating and Cr-graphite coating purpose. To prepare a fresh facing cylindrical surface for coating it is turned on a lathe. To protect other faces from being coated, a thin coating of neutral non conducting organic grease is applied and dried. All the sharp edges were rounded off to avoid burning during electroplating. The facing surface was finally cleaned with acetone to remove any grease on the surface.

#### **COATING PROCEDURE:**

Schematic diagram of the set up used in the present study is shown in the Fig.3.2. For chromium plating bath composition used is shown in table 3.1. For chromium graphite composite coating, powder particles to be codeposited were added into plating bath and blended for about 3-4 hours. This was done to ensure uniform suspension of particles in the bath. The stirring was continued throughout the plating period.

Hot water from the constant temperature bath was recirculated through the double walled glass vat containing the electroplating solution using a pump. When the required temperature was achieved the prepared specimen was placed in the plating bath with the help of a specimen electrode holder clamp. The anode was also lowered into the required current to pass in the circuit. Plating time was ten hours in all the experiments. Distilled water was added to make up for the evaporation losses.

#### **(3.4) MICROGRAPHS:**

Photographs of worn out flakes, wear tracks, and cross section of coatings were taken using scanning electron microscope.

### (3.5) WEAR TESTING

Amsler wear testing machine was used to study the properties of the composites prepared. Among two shafts meant for fixing specimens for testing wear, the sample holder (Fig.1) was fixed with the bottom shaft. Using gear manipulation the above shaft was freed from rotation and was fixed rigidly using a pin.

Heat treated pellet was fixed in the sample holder and machine was first adjusted to zero load ( following the instruction given in the manual of the machine ) and again adjusted to give 5 Kg load on the specimen. A to and fro motion of 3 mm was adjusted to be given by the machine in the axial direction.

A graph paper cut into proper size (16x11 cm ) was stuck on to the recording drum using a bit of glue. Machine was started the swinging bracket down i.e. the sample and the ring were not touching each other, or, in other words there was no load applied to the specimen, to see what was inherent torque given by the machine itself during operation. This was noted on the graph paper by drawing a line using the marker. When operated without sample, the integrating disc was adjusted not to rotate eventhough the disc on which the integrating disc was placed, rotated. ( i. e. the integrating disc was placed exactly at the centre of the disc ).

Fast paper feed ( ie fast rotation of recording drum ) was fixed to see clearly the changes of torque on the graph paper.

The swinging bracket was lifted up and the load of 5 kg was applied between the interfaces of specimen and the ring. After having noted the revolution counter reading, integrating disc counter reading, initial weight of the pellet and the time, machine was started and was kept in low speed point.

The torque range selected for measuring torque was 10 cm-kg and the speed of the wear path was found to be  $0.35 \pm 0.003$  m

-1  
s .

When the wear path was approximately 1Km the machine was put off, and the readings of counters, final weight of the specimen and the time, were noted down. The graph sheet on which torque changes were recorded was cut using a blade and taken away from on the recording drum.

#### CALCULATION OF DIFFERENT PARAMETERS

Amount of wear is calculated by finding the amount of loss of material from the specimen. The number of revolutions of the ring is equal to 10 times of the counter reading. Supposing N is the reading of the counter then 10 N is the number of revolutions made by the ring.

$$(i) \text{ Wear path } = L = 2 \times (3.14) \times r \times 10 \times N$$

where  $r$  = radius of the ring =  $34.8/2$  mm

$$= (3.14) \times 34.8 \times 10 \times N \text{ mm}$$

$$= 1.09327 \text{ N meter.}$$

Wear path  $L$  was calculated using above formula.

$$(ii) \text{ Wear path unit length} = w = \frac{W_1 - W_2}{1.09327N} \text{ g / m}$$

where  $W_1$  = initial weight of the specimen.

1

$W_2$  = final weight of the specimen.

2

The unit of  $W$  is g/m.

(iii) According to manual the work done by the specimen during one revolution =  $A = F \times S$

$$= p \times 2 \times (3.14) \times r$$

where  $p$  = load =  $m / r$

$m$  = momentary torque

$$A = m/r \times 2 \times (3.14) \times r = 2 \times (3.14) \times m$$

$r$  = radius of the specimen

$s$  = wear path per revolution.

This can be easily calculated by multiplying the integrating disc counter reading ( $N_i$ ) and the maximum torque possible (end value of torque scale).

$$A = N_i \times \text{end value of the scale} = m \text{ Kg.}$$

The above result is arrived at as follows ;

When the lower shaft rotates 100 times and when the torque is maximum ( $M$ ) ( i e 80 mm away from the zero point ) the integrating disc rotates two times on the disc. If the torque is not zero and also not maximum, the integrating disc makes

$$N_i = (2 \times (3.14) / M) \times m$$

revolutions on the disc. Where  $m$  = momentary torque,  $M$  = maximum torque (10 ( or ) 50 ( or ) 100 ( or ) 150) cm Kg.

Divide equation by  $M$  both sides. Now the R.H.S.

$$A/M = 2 \times (3.14) \times m/M$$

is nothing but reading of integrating disc counter i e  $N_i$ . Since

the sample has made 100 revolutions to give  $N_i$  reading and therefore  $A$  is now now work done in 100 revolutions.

$$A = \sum_i N_i \times M_i$$

We get A in m Kg instead of Cm Kg so

$$A = 100 N$$

Amount of work done per meter of wear path can be calculated by dividing A by L ie

$$\text{work done per meter} = A/L$$

(iv) Torque can be directly seen on the scale during wear. Otherwise it is calculated from the graph paper recording. The total length of scale is 80 mm which corresponds to the maximum torque possible (10(or)50(or)100(or)150 Cm Kg depending upon the chosen range). Each mm of graph sheet corresponds to a torque proportion. In the present case 1 mm corresponds to  $10 \text{ CmKg}/80 = 0.125 \text{ CmKg}$ . The distance from the reference line on the graph paper to the torque marked by the marker, is measured in mm and is multiplied with 0.125 to give the corresponding torque value in CmKg.

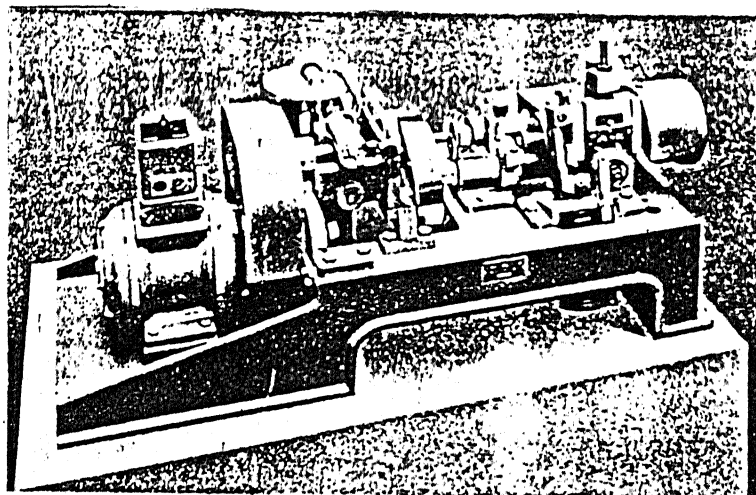
(v) Friction coefficient calculated using theory and formula.

$$\text{Friction coefficient} = \text{Torque} / p \cdot r$$

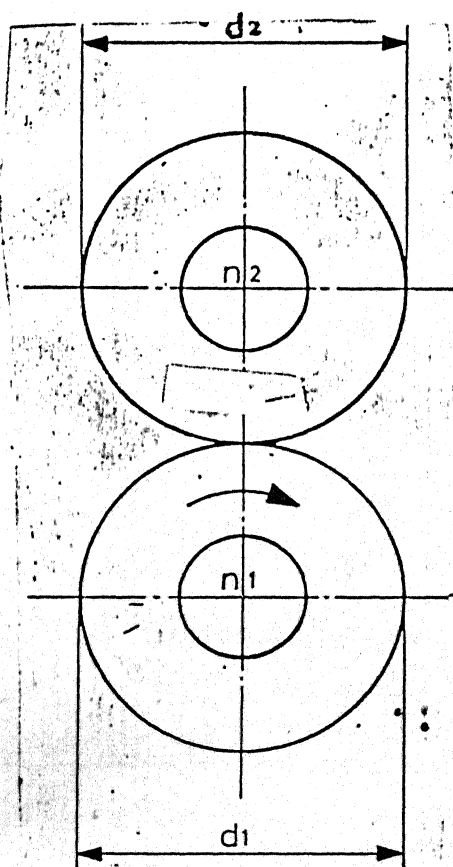
All the parameters were calculated using above theory and formula

Minimum and maximum torque range in which sample kept wandering around were calculated from recorded graph sheets.

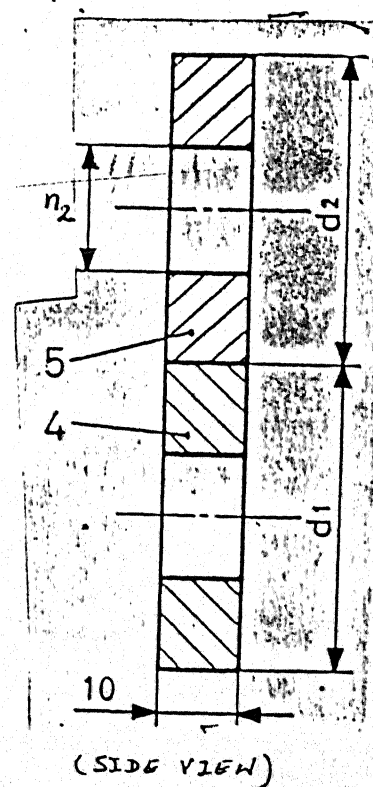




**AMSLER**  
TESTING MACHINES



(FRONT VIEW  
SAMPLE DIMENSION FOR  
SLIDING WEAR TESTING



$$\begin{aligned}d_1 &= d_2 \\n_2 &= 163 \text{ mm} \\n_1 &= 180 \text{ mm} \\t &= 10 \text{ mm}\end{aligned}$$

Fig: 31

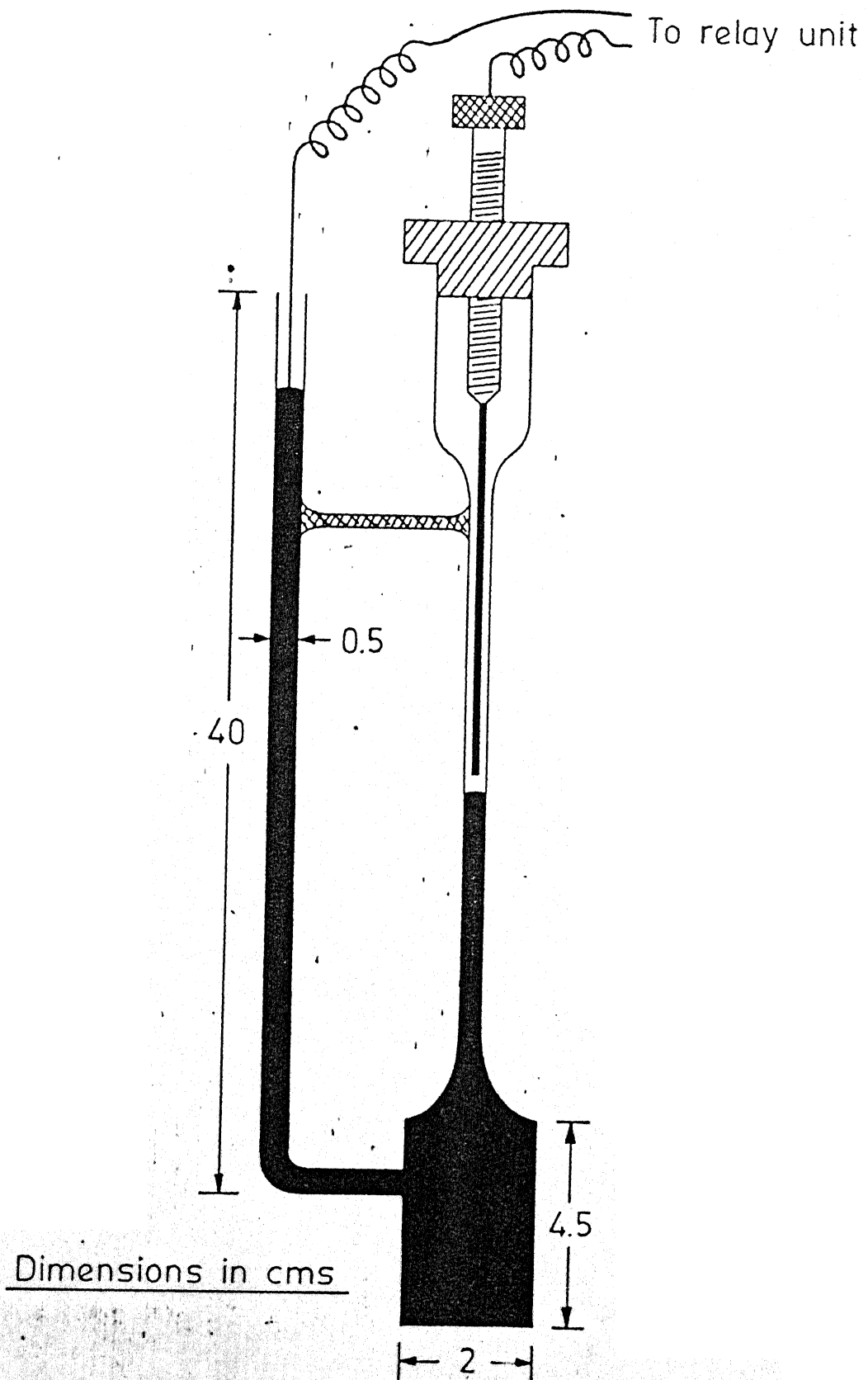


Fig. 3.2 Temperature controller for constant temperature water bath.

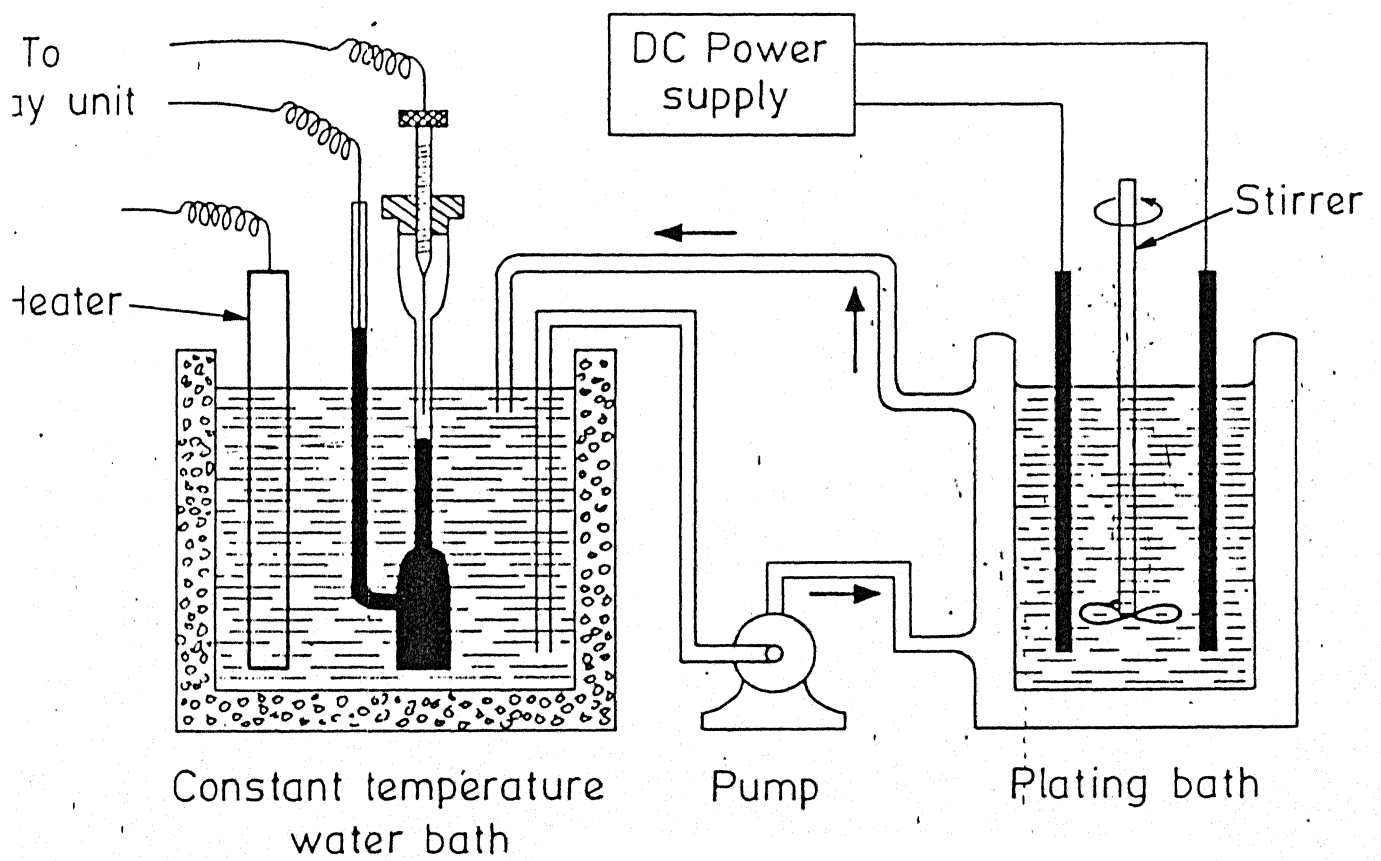


Fig. 3.3 EXPERIMENTAL SET - UP (schematic)

## CHAPTER 4

### RESULTS AND DISCUSSION

Wear experiment was performed on Amsler wear tesig machine of which schematic diagram with sample specification is showed in fig 3.1.

In the beginning experiment was performed with stationary sample made of bush material (carburized and heat treated low carbon steel) and rotating one of sprocket material (heat treated medium carbon steel).

Experiment was performed for three different time (i.e. 5 hrs, 10 hrs, and 20 hrs) and three different loads (50 kg, 100 kg, 150 kg). Important datas obtained for wear is shown in table 4.1 and values are plotted in different form in graph in graph section under different headings.

Cr-coating was performed on carburized heat treated low carbon steel. Coating specification is mentioned in Table 4.2 and scanning electron micrographs obtained is discussed later on. Here also same wear experiment is performed as in case of uncoated one and datas obtained is compiled under Table 4.3. Under graphs headings different graphs were plotted and discussed to considerable length.

Plates on Cr-graphite composite coating was performed which is discussed under SEM section. Here also wear experiment was performed.

Data obtained is discussed under Table 4.5. Here wear testing is performed only for one load i.e. 100 kg. Again different graphs were plotted and discussed under separate heading.

In the end wear study was performed for two sample made up of same material i.e. heat treated medium carbon steel. Datas obtained is compiled under Table 4.4 and related graphs plotted is discussed under separate headings.

CENTRAL LIBRARY  
I. I. T., KANPUR

Acc. No. **107887**

TABLE-4.1

SLIDING WEAR BEHAVIOR OF BUSH & SPROCKET IN UNCOATED CONDITION

Load (kgs)	Time (hrs)	Weight Loss		N	Wear Path (1.09327*N) mts	Wear/Length <sup>-5</sup>	
		Bush	Sprocket			Bush	Sprocket
50	5	0.0882	0.1127	5808	6349.7	1.39	1.77
50	10	0.1811	0.1852	7697.5	8415.4	2.15	2.20
50	15	0.3142	0.3332	17561.5	19199.5	1.64	1.73
50	20	0.6253	0.4064	22726	24845.6	2.5	1.64
100	5	0.5046	0.15065	5876	6424	7.85	2.34
100	10	0.7023	0.2734	11780	12878.7	5.45	2.12
100	15	0.7858	0.4866	18040	19722.6	3.98	2.46
100	20	1.0234	0.5973	22826	24955	4.1	2.39
150	5	1.2847	0.1886	5896	6445.9	19.93	2.9
150	10	2.0246	0.3216	11598	12680.0	15.96	2.54
150	15	2.5556	0.64	17685	19334.48	13.22	3.31

TABLE-4.2

Cr-Coating on Bush Steel Sample

Initial Weight of the Sample (W) <sub>i</sub> =	56.7871 gms.
Final Weight of the Sample (W) <sub>f</sub> =	57.3813 gms.
Total Weight of coating obtained (W) =	0.5942 gms.
Initial Outer diameter (D) <sub>i</sub> =	34.72 mm.
Final Outer diameter (D) <sub>i</sub> =	38.40 mm.
Thickness of the coating (D/2) =	1.84 mm.
Width of the sample (t) =	10.0 mm.
Applied Current (I) =	6.2 amp.
Coating time =	10.0 hrs.

TABLE- 4.3

SLIDING WEAR BEHAVIOR OF BUSH-SPROCKET MATERIAL IN  
Cr-COATED CONDITION

Load (kgs)	Time (hrs)	Wear-Weight Loss (gms)		(N)	Wear-path (1.09327*N) (mts)	Wear/Length <sup>-5</sup> (gms/mt)x10	
		Bush	procket			Bush	Sprocket
50	5	0.0864	0.1349	5936	6489.65	0.56	2.1
50	10	0.1297	0.2790	11933	13046.0	1.0	2.1
50	15	0.1851	0.5336	17388	19010.0	1.0	2.8
50	20	0.3122	0.6245	23330	25506.0	1.2	2.4
100	5	0.4036	0.2001	5946	6500.6	6.2	3.1
100	10	0.5452	0.3545	12810	14004.8	3.9	2.53
100	15	0.5663	0.6040	17411	19034.9	2.97	3.17
100	20	0.8098	0.7338	22840	24970.3	3.2	2.9
150	5	0.6438	0.2653	5900	6450.3	10.0	4.1
150	10	1.0268	0.4300	11372.5	12433.2	8.2	3.4
150	15	1.1672	0.4743	17685	19334.5	6.0	2.4
150	20	1.5267	0.7632	22816.5	24944.6	6.1	3.0

TABLE-4.4

SLIDING WEAR BEHAVIOR OF HEAT-TREATED MEDIUM CARBON STEEL  
(Both sample made of same material)

Load(kgs)	Time (hrs)	Wear Weight Loss (gms)	
		Bush	Sprocket
100	5	0.3045	0.1723
100	10	0.4087	0.4376
100	15	0.6763	0.6060
100	20	0.8399	1.4456

---

TABLE-4.5

SLIDING WEAR BEHAVIOR OF BUSH-SPROCKET MATERIAL IN Cr-GRAPHITE  
COMPOSITE COATED CONDITION

---

Load (kgs)	Time (hrs)	Wear-Weight Loss (gms)	
		Bush	Sprocket
100	5	0.3146	0.4712
100	10	0.4519	0.6207
100	15	0.4727	0.8723
100	20	0.7158	1.0022

---



#### (4.1) GRAPHS

##### 1. D1A:- WEIGHT LOSS VS TIME (STATIC: CARBURIZED)

This graph deals with the wear study of low carbon bush steel which is carburized, quenched and then tempered at 150 C to achieve 100 % Martensite. Here for higher load (i.e. 150 kg), initial wear rate is very high then it continuously decreases.

For medium and low load (i.e. 100 kg & 50 kg) initially wear rate is higher then decreases then finally it again increases.

Initially wear rate is higher because of higher surface roughness and higher stress due to small surface area in contact. As time progresses from adhesion theory to delamination theory takes over predict wear mechanism according to which wear rate is mainly controlled by subsurface void nucleation and crack propagation. Due to frictional energy loss heat generated is used in forming oxide glaze which gets embedded on the surface which in turn restricts surface wear loss. Curve shows three distinct regions called threshold region, steady growth region and static mode region respectively.

##### 2.D1B: WEIGHT LOSS VS TIME: (ROTATING : Against carb.)

This graph deals with the wear study of rotating sprocket sample which is medium carbon steel quenched and tempered to get 100 % martensite. It is sliding against carburized static bush sample.

Here for all load (i.e. 150, 100, 50 kg) initially wear rate is higher then relatively lower then again higher and finally lower.

Initially wear rate is higher and then lower due to the same reason as it is in the case D1A. Here difference in wear mechanism with respect to D1A case is due to change in loading pattern. In rotating sample due to different faces coming in contact there is cyclic loading taking place which leads to fatigue mode of failure. Finally in the end wear rate decrease because of the basic microstructural difference of medium carbon with respect to low carbon steel.

##### 3.DL1A: WEAR LOSS VS LOAD (STATIC: CARBURIZED)

This graph is wear loss vs load graph at different time for bush material. With increase in time there is net shift in graph towards higher wear loss which looks obvious.

With increase in load there is continuous increase in wear loss which is partly clear from the graph but since experimental



34  
data could only be obtained for a few load a continuous graph is not plotted.

As load increases, frictional force also increases even for constant frictional coefficient which leads to higher wear loss. Higher load also helps in easy void nucleation and faster crack growth which is one of the important mechanism of controlling wear loss.

#### 4. DL1B: WEIGHT LOSS VS LOAD (ROTATING : Against carb.)

This graph is for sprocket material sliding against bush material. Again there is net shift towards higher wear loss with increase in time. With increase in load wear loss continuously increases.

#### 5. D2A. WEIGHT LOSS VS TIME (STATIC: Cr Coated)

Here bush material is Cr-coated. Thickness of Cr-coating developed is considerable as it is evident from plate-19. Here again three stage wear mechanism is the same as it is in D1A case. Weight loss vs time graph should be continuous but that could not be plotted with higher accuracy because data are available for limited time interval and for few number of loads only. But still three stages of crack propagation i.e. threshold region. Steady growth region and static mode region is evident from the graph.

#### 6. D2B: WEIGHT LOSS VS TIME (Rotating: Against Cr-coated)

Here sample made of sprocket material is sliding against bush material which is Cr-coated. Wear mechanism is similar to four stage wear mechanism of graph D1B. Here also in the beginning there is a faster rate of wear, then it is slowed down and then again higher up and finally slowed down.

#### 7. DL2A: WEIGHT LOSS VS LOAD (Static: Cr-coated)

Bush material is Cr-coated. Nature of graph is similar to DL1A and reason of variation of wear rate with load is also almost the same. Wear rate is continuously increasing with increasing load and with increase in time there is net upward shift towards higher wear loss.

## 8.DL2B. WEIGHT LOSS VS LOAD (Rotating: Against Cr-coating)

Here sprocket material is sliding against bush ~~one~~ with Cr-coating. Nature of graph is similar to DL1B. There is continuous increase in wear ~~rate~~ with increase in load and with increase in time, whole curve shifting towards higher wear rate.

## 9. D4A: WEIGHT LOSS VS TIME (Load 100 kg, Static: Heat)

This is for bush sample which is made of material earlier used for sprocket i.e. medium carbon steel quenched and tempered to get 100 % martensite. Wear mechanism is of four steps type as it is for sprocket sample made of same material dealt within D1B graph. But as important difference is that here no cyclic loading is taking place and so four stage wear mechanism is not due to fatigue but due to microstructural difference. This sample is different from carburized low carbon steel which is quenched and tempered to get 100% martensite. In later case the surface martensite is of higher carbon type but as we go inside it is of low carbon type. But in earlier case i.e. in case of medium carbon steel there is only one type of martensite uniformly distributed ~~load~~ all over the sample.

Here in the beginning adhesion mechanism ~~the~~ controls wear rate but later on it is taken over by delamination mechanism which now start controlling the wear rate. Initially at void nucleation stage wear rate is lower which increases in the steady ~~graph~~ region but later on it again decreases due to almost complete diminution of surface wear loss. Thus in the end only sub-surface wear loss mechanism is the rate controlling factor

## 10.B4B: WEIGHT LOSS VS TIME (LOAD -100 kg:Rotating: Againstheat)

This graph is for rotating sprocket sample part which is made of the same medium carbon steel as bush material is in D4A or earlier sprocket material. Thus in this case bush and sprocket both are made of same material and one is sliding over the other.

There is fundamental shift in wear phenomenon in the sense that initial wear rate is lower and it increases then decreases and finally for longer time it increases very rapidly. Since tempered medium carbon steel has very coherent microstructure in comparison to carburized one and it is a case of two similar surfaces sliding against each other and its surface is comparatively smoother, so surface adhesion wear which is initially rate controllling is comparatively low. For as time progresses delamination wear takes over which becomes rate controlling and so wear rate decreases. In third stage there is fall in wear rate not because of lowering of delamination wear which get into a steady stage region, but because of total loss of adhesion wear which almost becomes negligible in later stage. In the last stage there is a rapid rise in wear rate due to

fatigue failure of the sample.

#### 11. D5A: WEIGHT LOSS VS TIME (Load-100 kg:Static, Cr-graphitecoating)

This graph is for bush sample again made of low carbon steel which is carburized quenched and then tempered to get 100% martensite. Here Cr-graphite composite coating is performed to provide solid lubrication and to enhance wear resistant efficiency of bush-sprocket arrangement.

This is a standard three stage graph common to most of the bush material failing under crack propogation mechanism which is extensively dealt in literature survey part and in case of graph D1A. Again graph should have been continuous but since experiment could be performed only for few time intervals and one load (i.e 100 kg) continuous graph is not plotted.

#### 12 D5B: WEIGHT LOSS VS TIME (Load 100 kg: Rotating ; Against Cr-graphite comp)

This graph is for sprocket material which is sliding against composite coated bush sample.

This is a standard four stage graph common to most of the sprocket material and it is extensively dealt earlier in D1B and other cases.

#### 13. D3A: WEIGHT LOSS VS TIME (STATIC: CARB. COAT)

This is a master graph for bush sample. One set of sample is simply low carbon steel, carburized,quenched then tempered to get 100% matremsite. In other one Cr-coating is performed over initial bush material.

Wear testing is performed for three different loads i.e.50kg 100 kg, and 150 kg and for two materials mentioned above. This is a sum graph of D1A and D2A and here relative advantage of Cr-coating over uncoated sample can be clearly understood. Here initial advantage obtained over uncoated one is maintained all over with the same difference. As it is evident from plate 19,20 & 21 that coating improves the surface finsih and immensely reduces initial adhesive wear loss. After coated part wears out rest of the wearing process is similar for both the cases because now materials sliding over the other are the same.

#### 14. D3B: WEIGHT LOSS VS TIME (Rotating: Against carb.:Cr-coated)

This is a master graph for sprocket material which medium carbon steel quenched and tempered to get 100% martensite. In one

set this is sliding against bush material which is low carbon steel carburized quenched and tempered for 100% martensite. In another set original bush is Cr-coated and our sprocket sample sliding against it.

Wear testing is again performed at three different load i.e. 150 kg, 100 kg and 50 kg. Basic mechanism of wear is discussed in D1B and D2B. Here comparison of relative wear loss would be easier. Here again initial advantage gained over the other is maintained. For sample sliding against Cr-coated bush sample wear loss is higher because it is facing relatively harder surface. On the other hand for the sprocket sample, sliding against uncoated bush sample wear loss is relatively smaller. For higher load (i.e. 150 kg) even against uncoated bush sample for longer time wear increases with a faster rate. But for lower load (i.e. 100 kg and 50 kg) it is otherway round.

#### 15. DL3A: WEIGHT LOSS VS LOAD (STATIC CARB.:Cr-coated)

This is a master graph for bush sample one set for uncoated one and another one for Cr-coated. Graph is plotted for three different time intervals i.e. 5 hrs, 10 hrs, 15 hrs. Mechanism is already discussed in DL1A and DL2A and here is a sum of these two sets. For all load and time interval wear rate with respect to load is always higher than Cr-coated one.

#### 16. DL3B WEIGHT LOSS VS LOAD: (Rotating against carb. Cr-coat)

This is a master graph for sprocket material. One set of graphs is for sprocket material sliding against uncoated bush sample and another set for sliding against Cr-coated one.

For any particular interval wear rate against coated sample is always higher than uncoated one, but if two different time interval are compared then it is not the case. In fact with changing time wear rates against Cr-coated and uncoated vary alternately.

#### 17. D6A: WEIGHT LOSS VS TIME (Load 100 kg : Static carb, Cr-coated Heat comp)

This is a master graph for bush sample having bush material itself replaced by medium carbon steel quenched and tempered to get 100% martensite. In other three cases one is where bush material is used as such in uncoated condition, in next one Cr-coating is done and in the last one Cr-graphite composite coating is performed.

Uptil 10 hrs of wear testing medium carbon steel gives the best result, but overall for longer time of wear Cr-graphite composite coatings on low carbon steel give the most satisfactory result.

4

18.: D6B WEIGHT LOSS VS TIME (Load-100 Kg: Rotating against carb, coat., heat comp.)

This is a master graph for sprocket material which is sliding against bush sample with different surface except in one case where bush and sprocket material are of the same medium carbon steel type. Uptil 15 hrs medium carbon steel gives fairly good performance for both as bush and sprocket material. Against composite coating wear rate of sprocket material is generally maximum. But for longer time wear rate of medium carbon steel overtakes wear rate of sprocket material which is again medium carbon steel against Cr-graphite composite coated one.

19.B1: WEIGHT LOSS VS TIME: (Static uncoated, Cr-coated)

This bar diagram is a relative comparison of wear rate of Cr-coated bush material with uncoated one.

For all load and time Cr-coated sample shows more wear resistance than uncoated one. For higher time of wear testing relative wear resistance gain keep on increasing.

20.B2: WEIGHT LOSS VS TIME: (Rotating : Against carb. Cr-coat)

This bar diagram is a relative comparison of wear loss of sprocket material sliding against carburized in one case and against Cr-coated one in the other.

Sample sliding against Cr-coated wear rate is always higher than sample sliding against uncoated one but as time of wear testing increases this gap gets healed up and for higher load and longer time of testing this difference is very less.

21.B3: WEIGHT LOSS VS LOAD (Static: Cr-coated, carb.)

This bar diagram is about relative wear study bush material in Cr-coated and uncoated condition. With increasing load and time gap between wear rate of coated and uncoated one keep on increasing. Times for higher load coating give even better performance even if wear time is extended.

22. B4: WEIGHT LOSS VS LOAD (Rotating: Against carb. Cr-coated)

This bar diagram is about relative wear study of sprocket material which is sliding against uncoated and Cr-coated bush sample.

Wear rate against Cr-coated one is always more than against



41.  
uncoated one with both increase in load and time. But for higher load and time this gap continues to decrease and for 150 kg load and 15 hrs testing time this difference is almost negligible.

23.B5: WEIGHT LOSS VS TIME (Load-100kg: Static:Carb.  
Cr-Coated,Heat,Comp)

This is a relative wear rate comparison bar diagram at 100 kg load for bush material under uncoated, Cr-coated, Cr-graphite composite coated and medium carbon steel sprocket material used for both sample condition.

For lower wear time heat treated medium carbon steel used for both sample giving the best performance but for longer wear times Cr-graphite composite coated one comes out to be the best alternative. Even for longer wear time heat treated medium carbon steel used for both sample will give better performance than uncoated carburized and then heat treated low carbon steel.

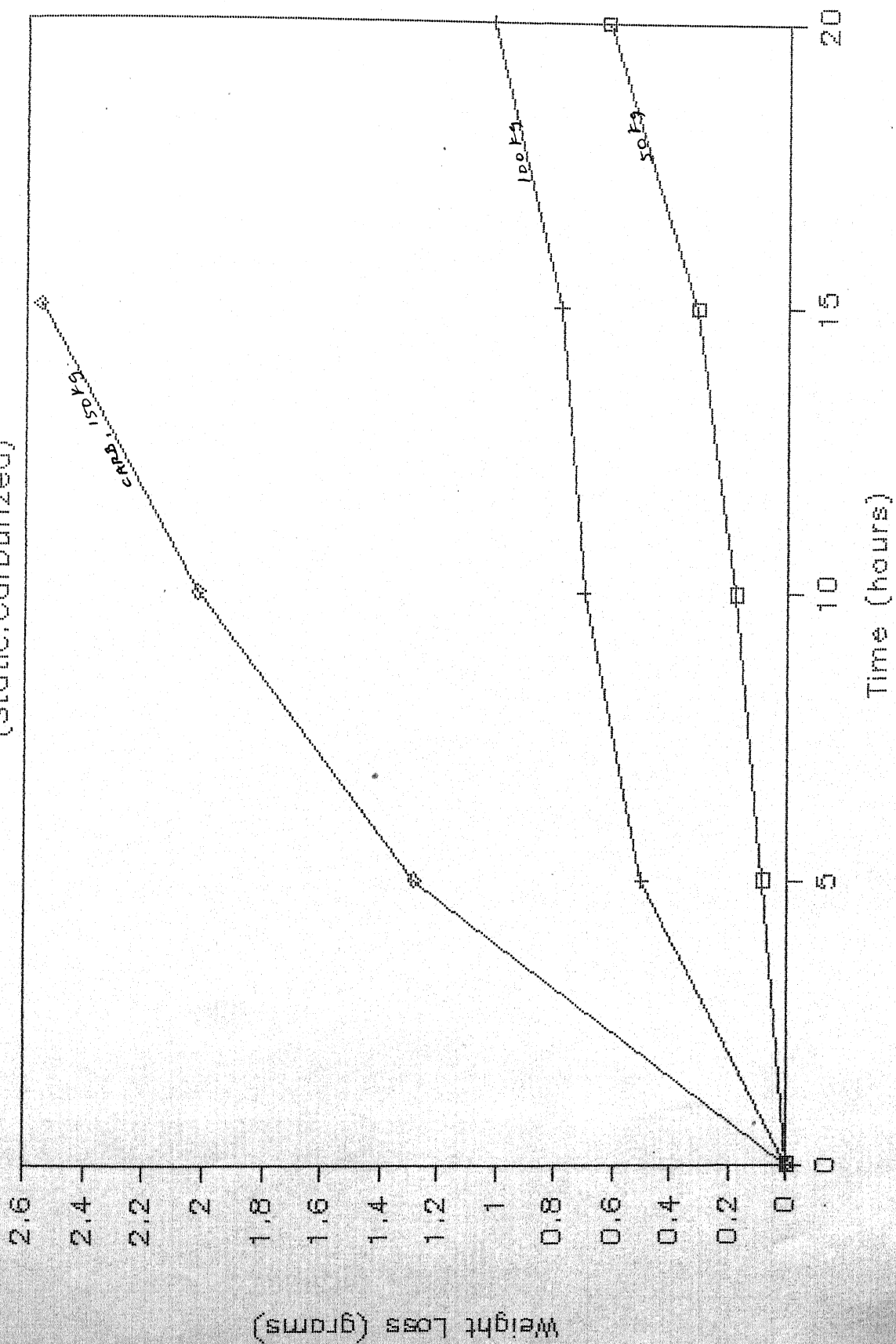
24.B6: WEIGHT CHANGE VS TIME (Load-100 kg,Rotating: Against  
Carb.Coat, Heat,Comp)

This is relative wear rate comparison bar diagram for sprocket sample which is heat treated medium carbon steel and is sliding against uncoated, Cr-coated, Cr-graphite composite coated and of same material as sprocket is made up of.

In general for uncoated one wear is the least for all cases but with increase in load and time difference between wear rate of uncoated and other surface treated one decreases except in the case of heat treated medium carbon steel where in the beginning this gap is almost negligible but with progress of time this gap increases very rapidly.

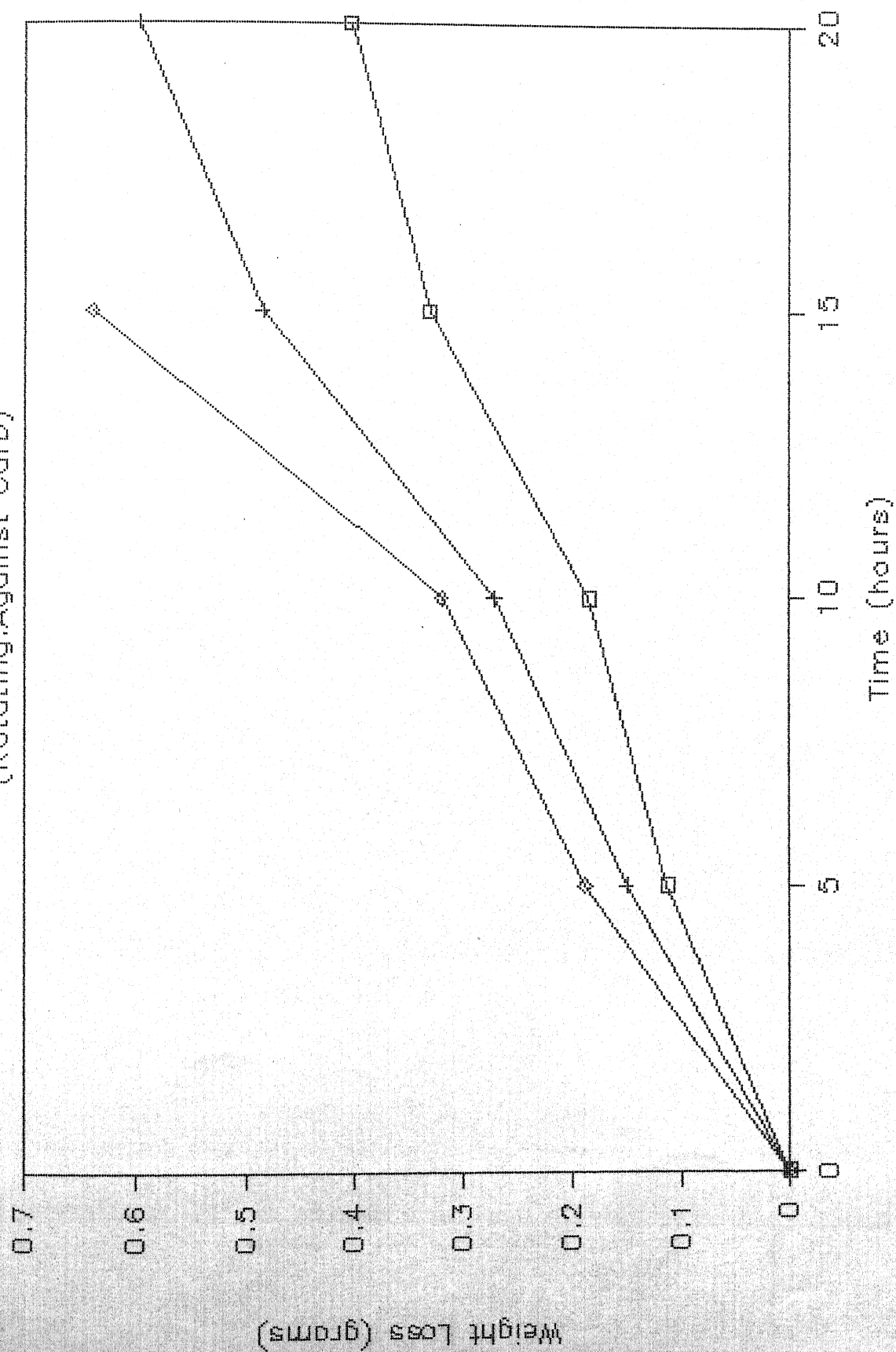
# WEIGHT LOSS V\ S TIME

(Static: Carburized)



# WEIGHT LOSS VS TIME

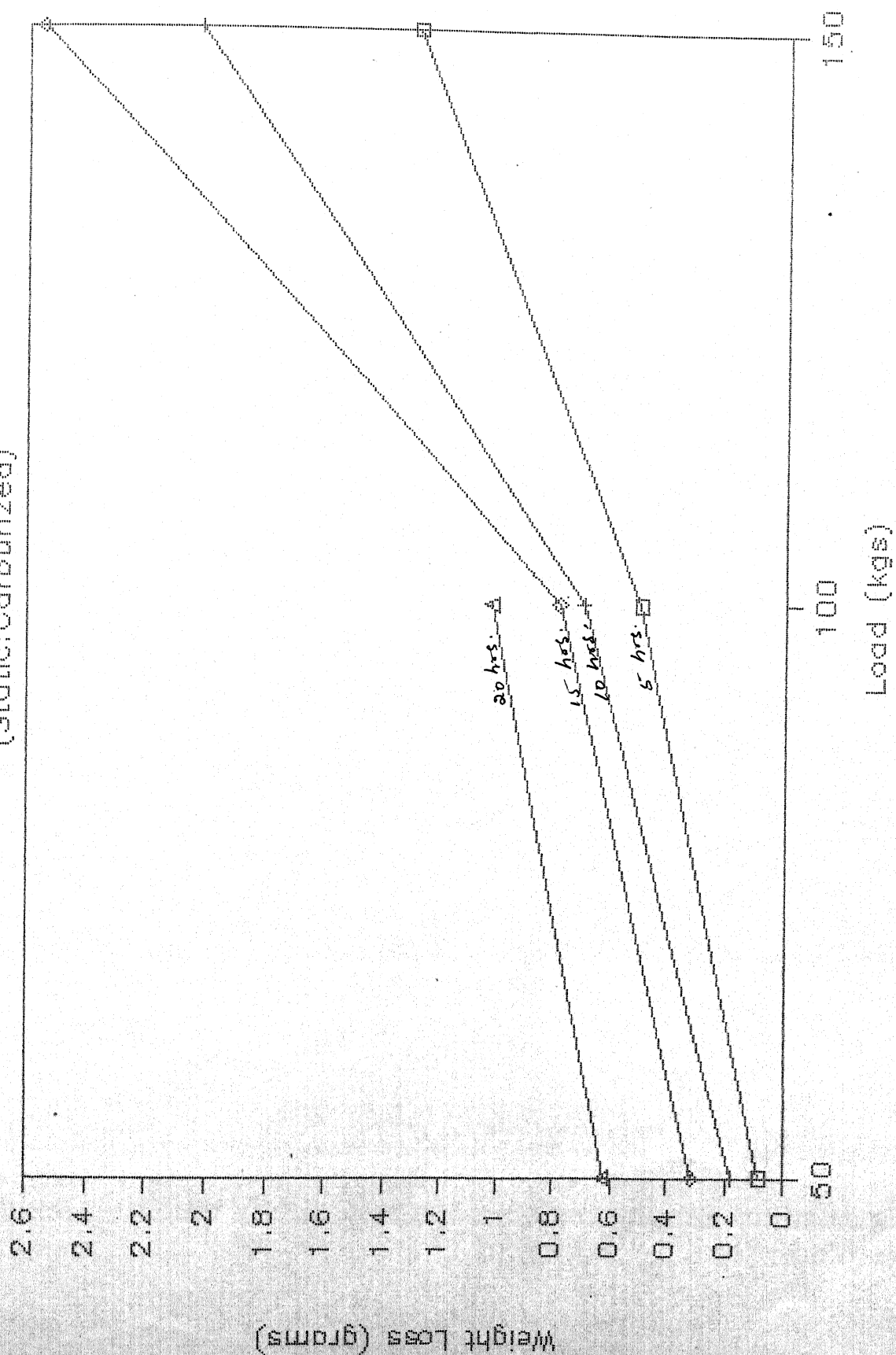
(Rotating: Against Carb)



2 DIB



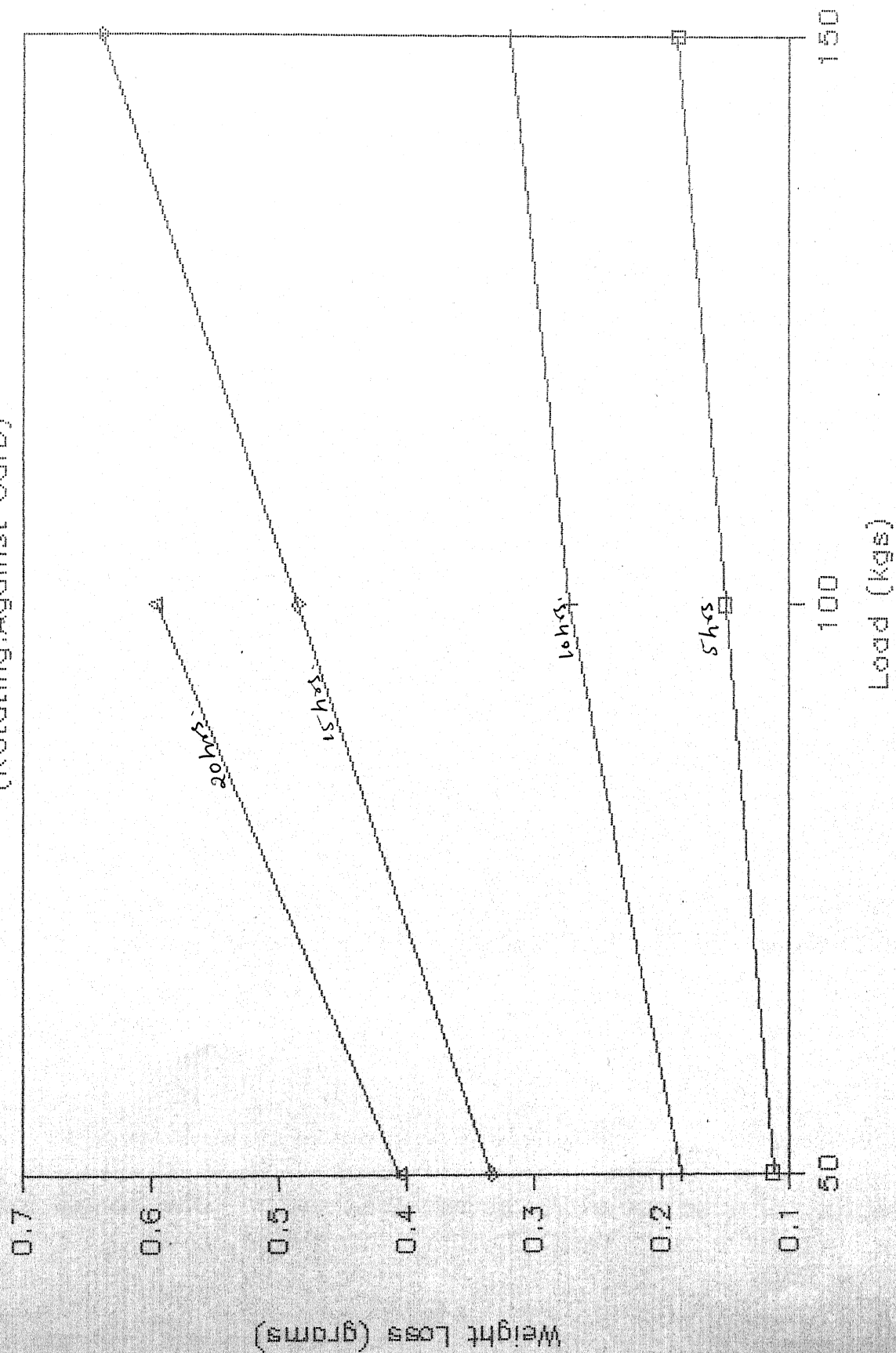
# WEIGHT LOSS VS LOAD (Static:Carburized)



3.DL1A

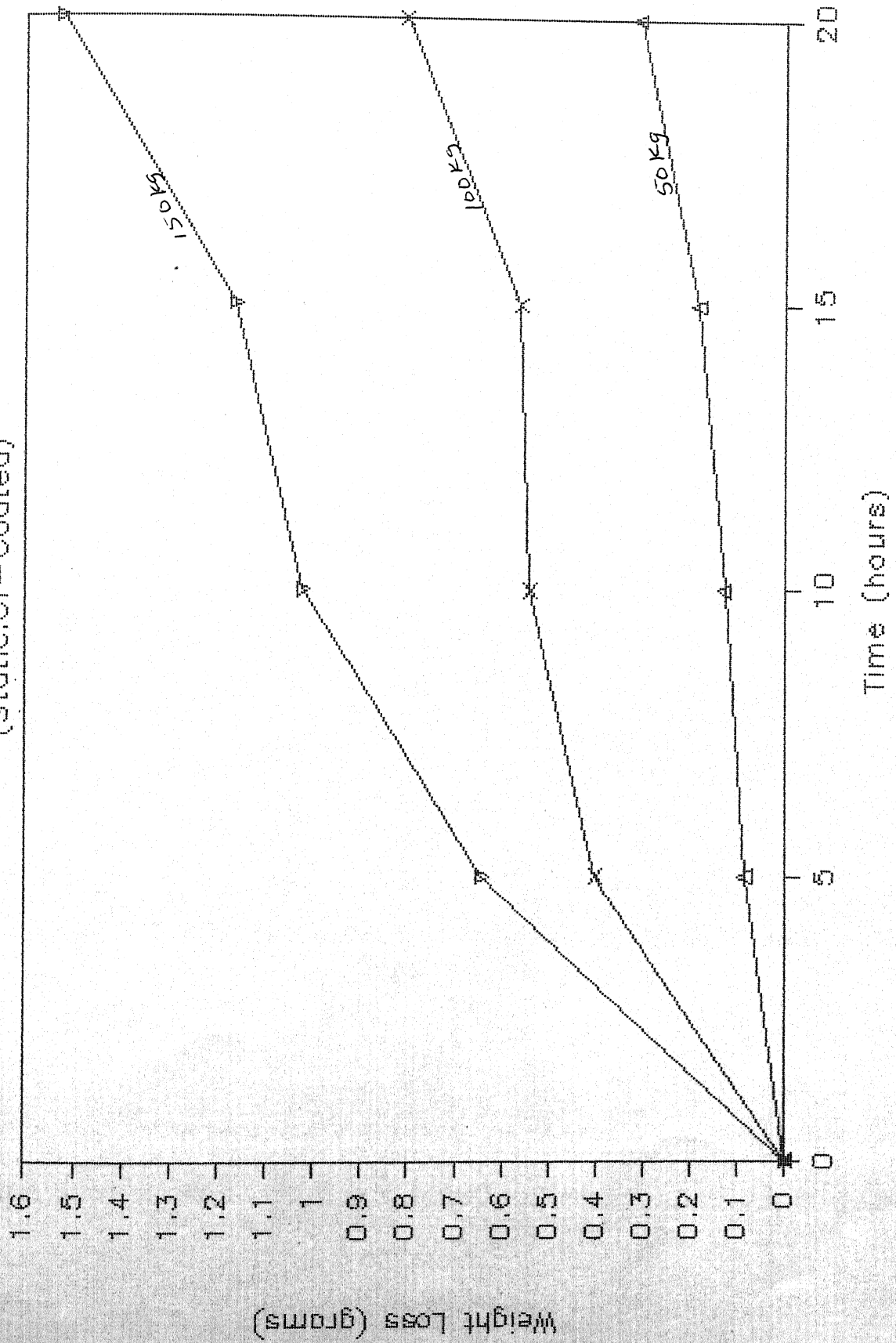
# WEIGHT LOSS VS LOAD

(Rotating Against Carb)



4-DL1B

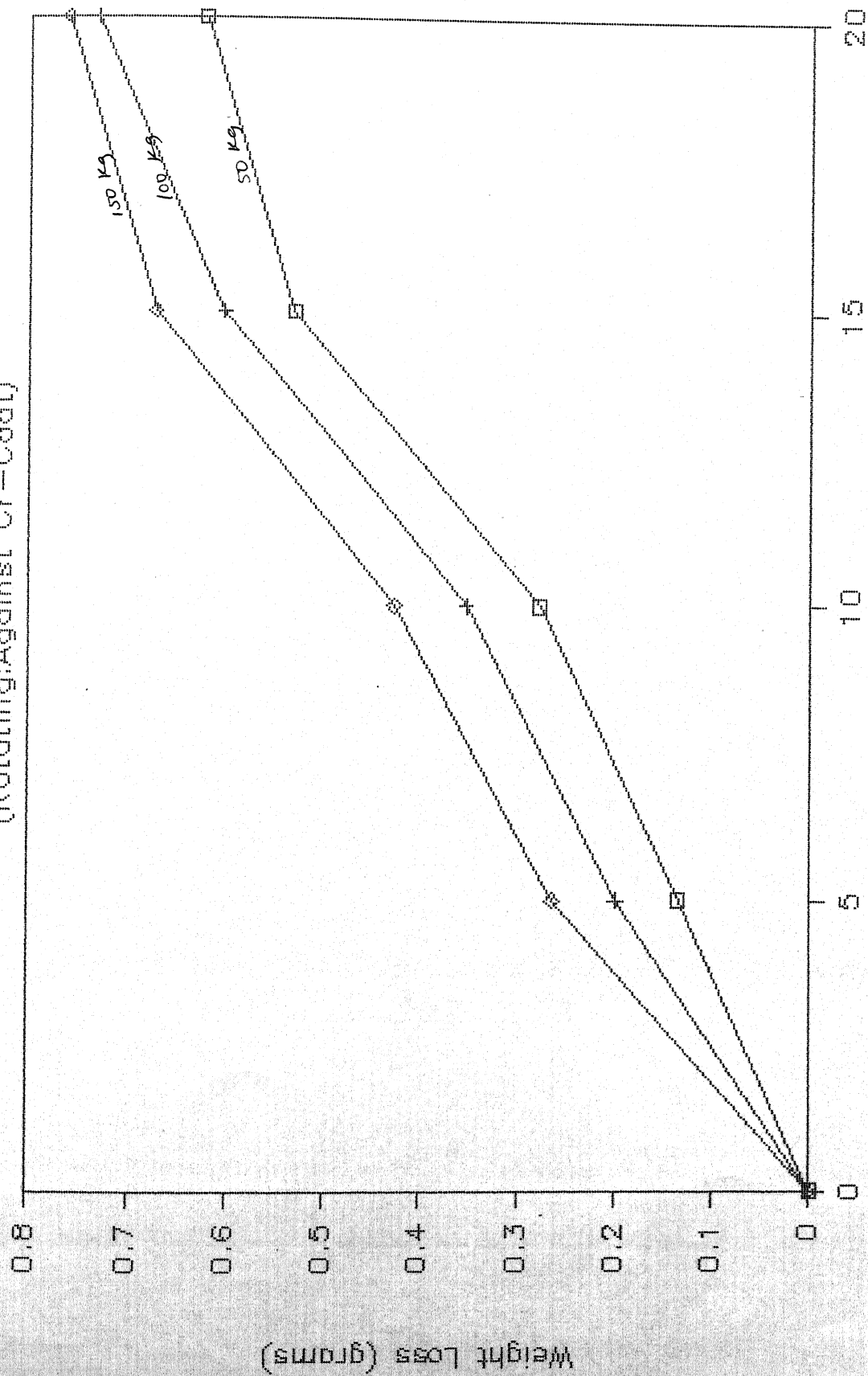
# WEIGHT LOSS V\ S TIME (Static:Cr-Coated)



5.D2A

# WEIGHT LOSS VS TIME

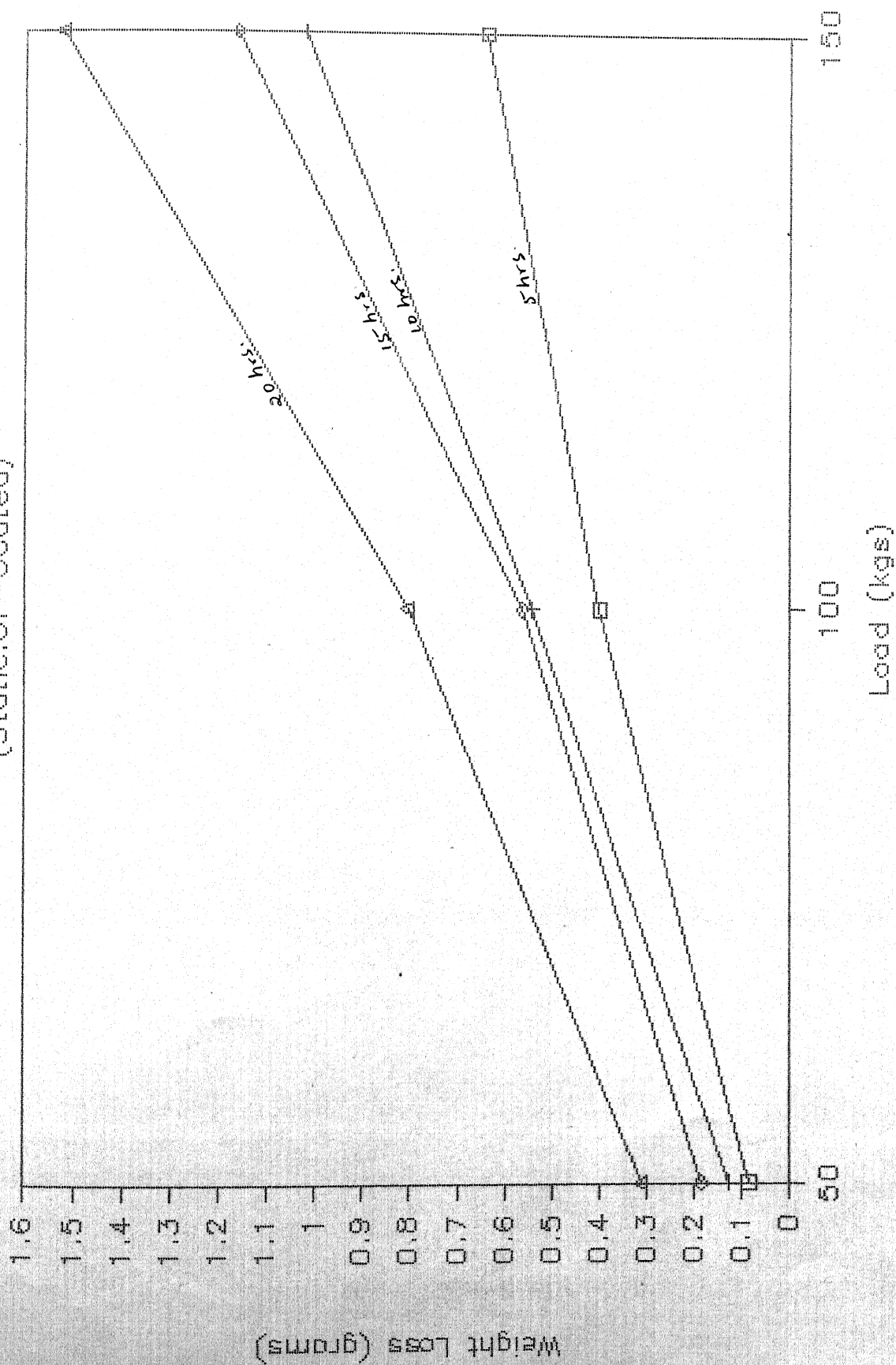
(Rotating Against Cr-Coat)



Time (hours)

6.D2B

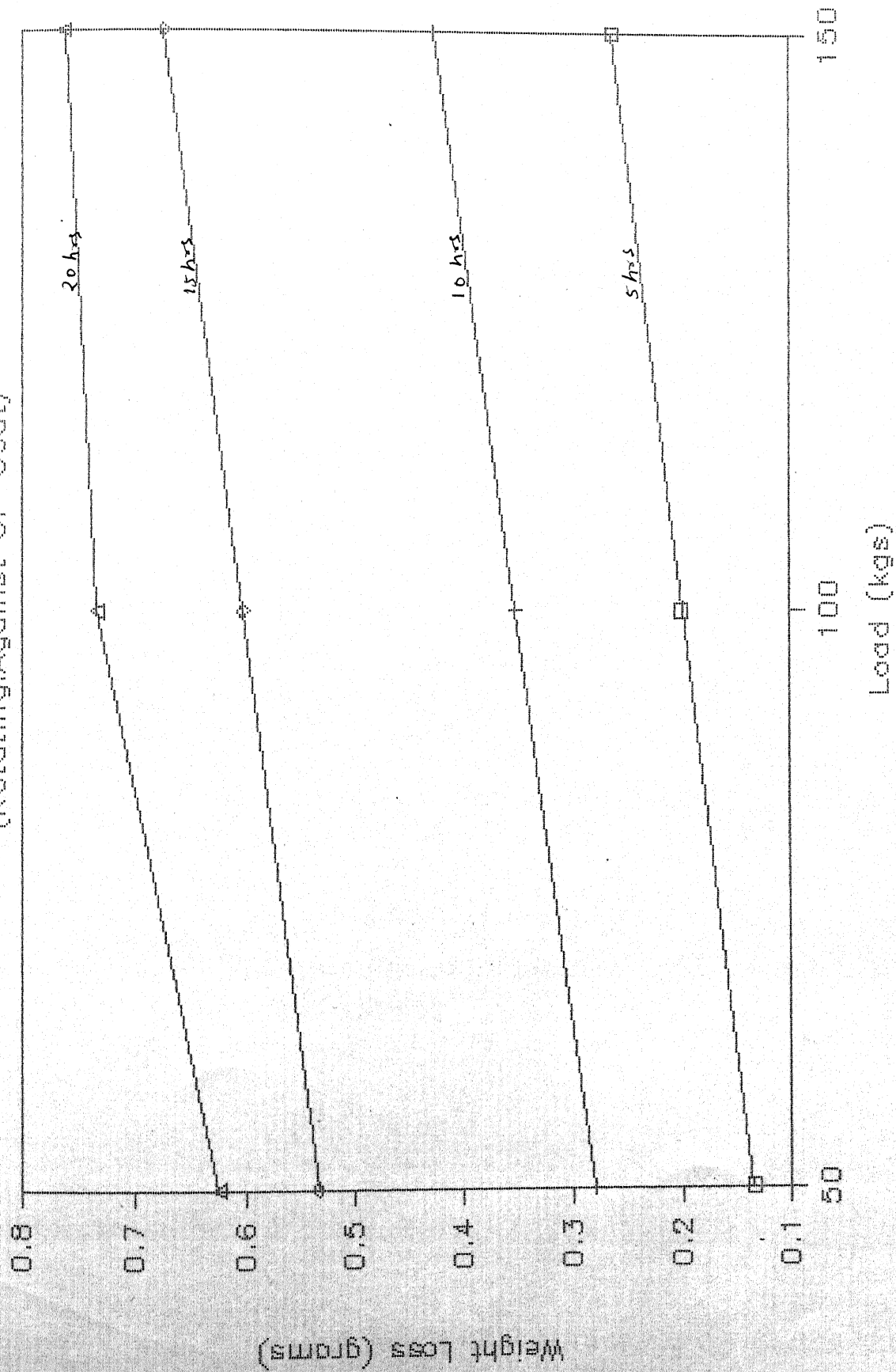
# WEIGHT LOSS VS LOAD (Static:Cr-Coated)



7-DL2A

# WEIGHT LOSS VS LOAD

(Rotating Against Cr-Coat)

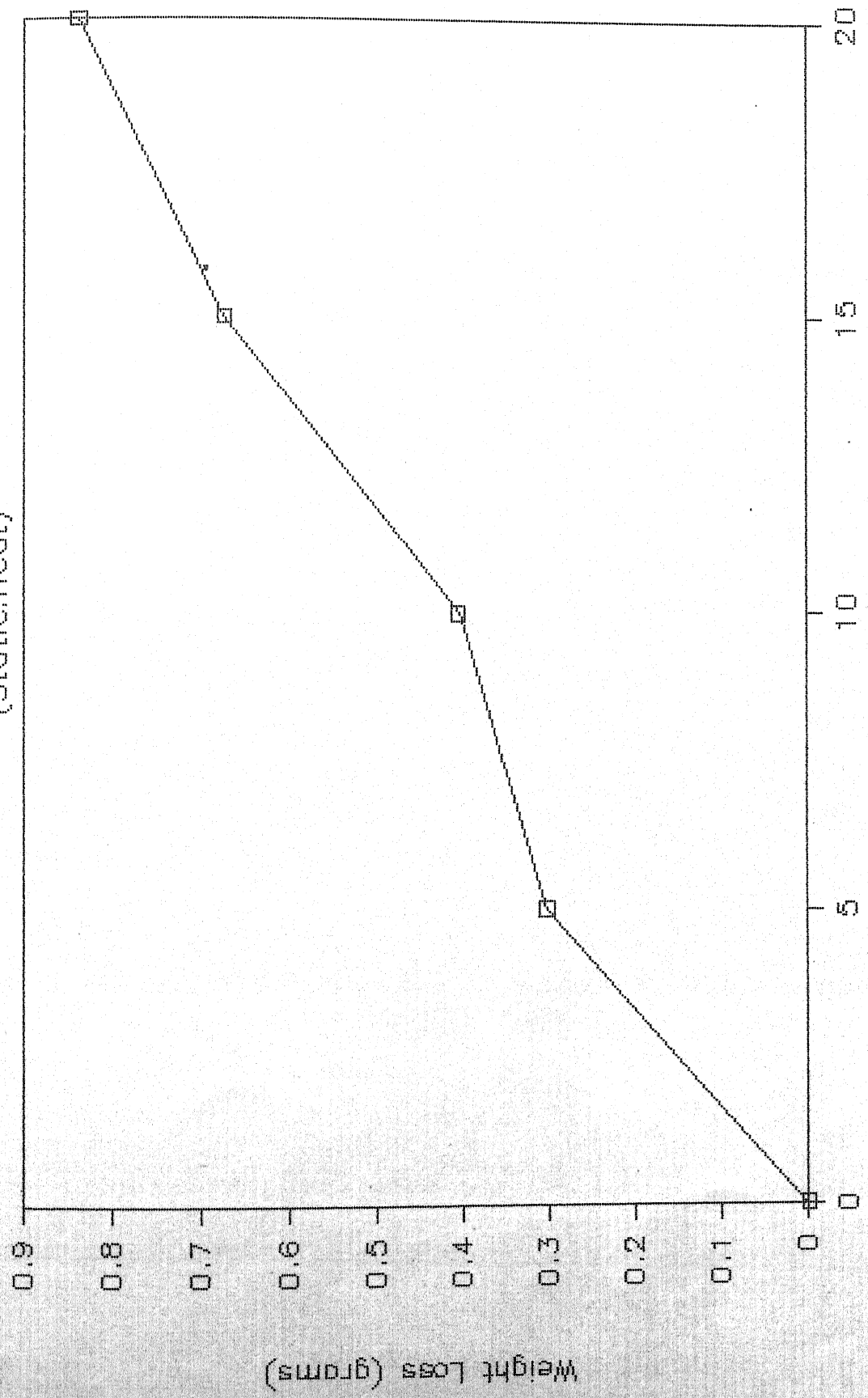


R.DL 2B



# WEIGHT LOSS VS TIME (Load-100 kg)

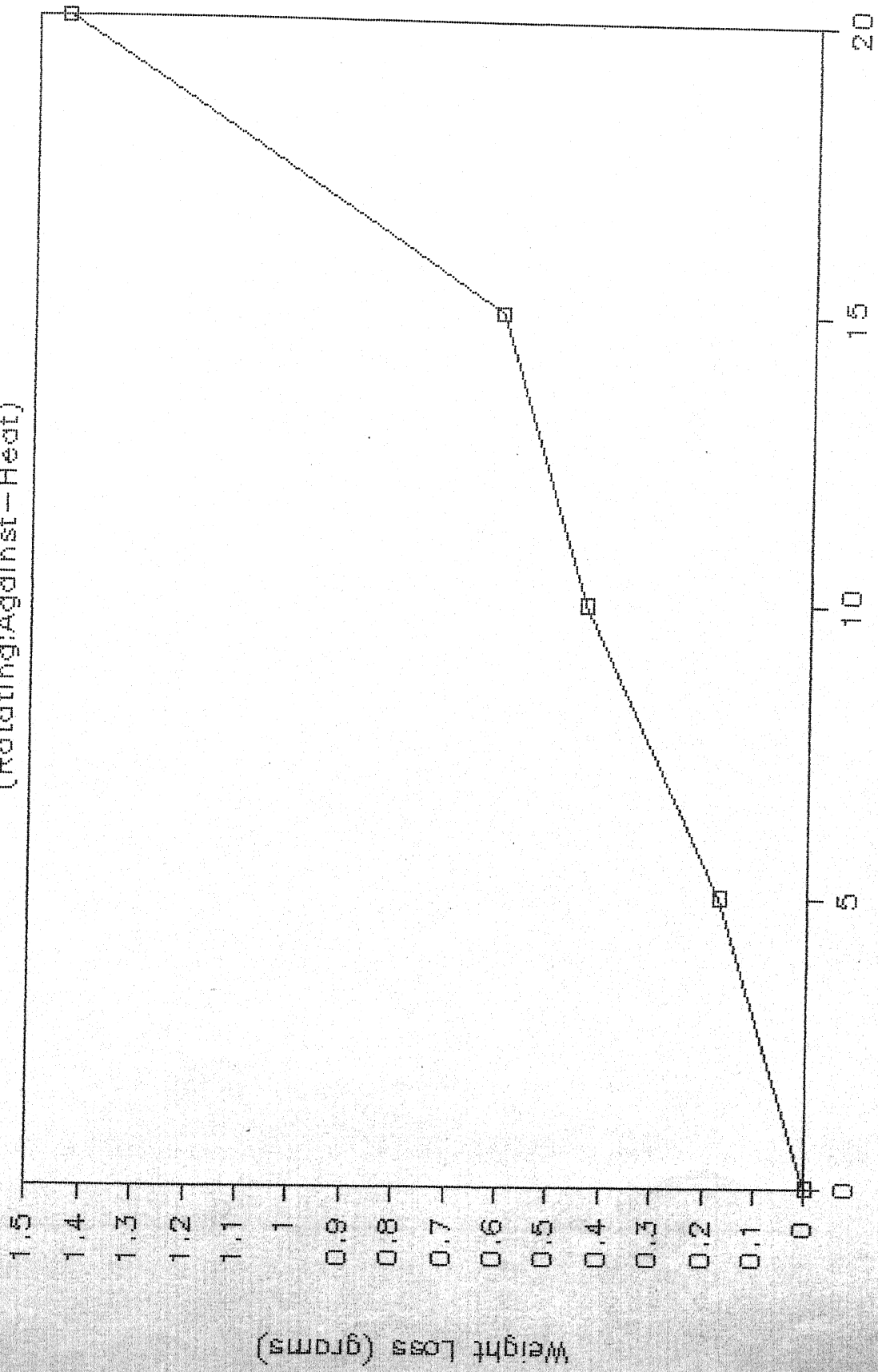
(Static:Heat)



Time (hours)

9.D4A

# WEIGHT LOSS VS TIME (Load—100 kg) (Rotating Against—Heat)

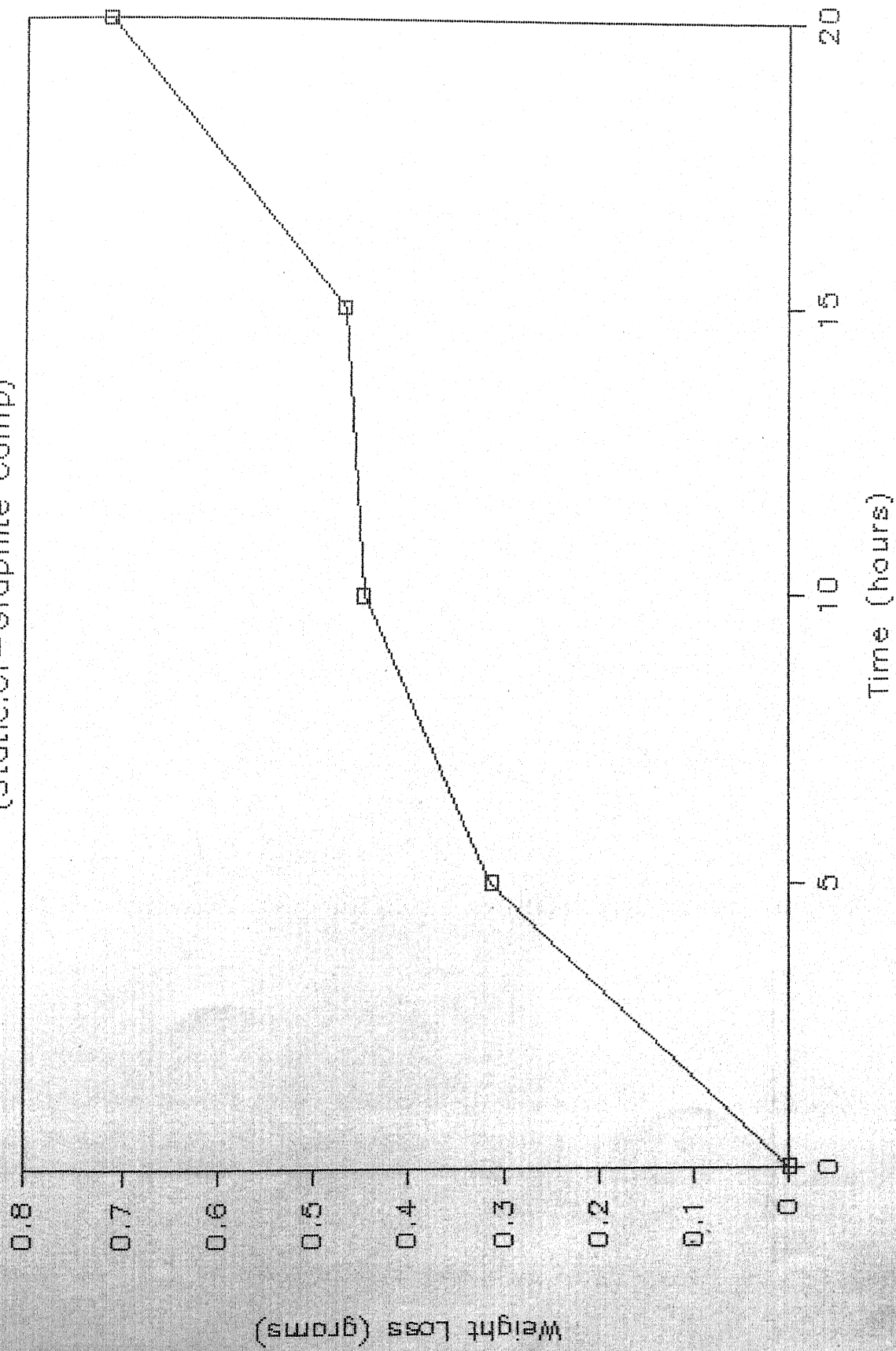


Time (hours)

10-D4B

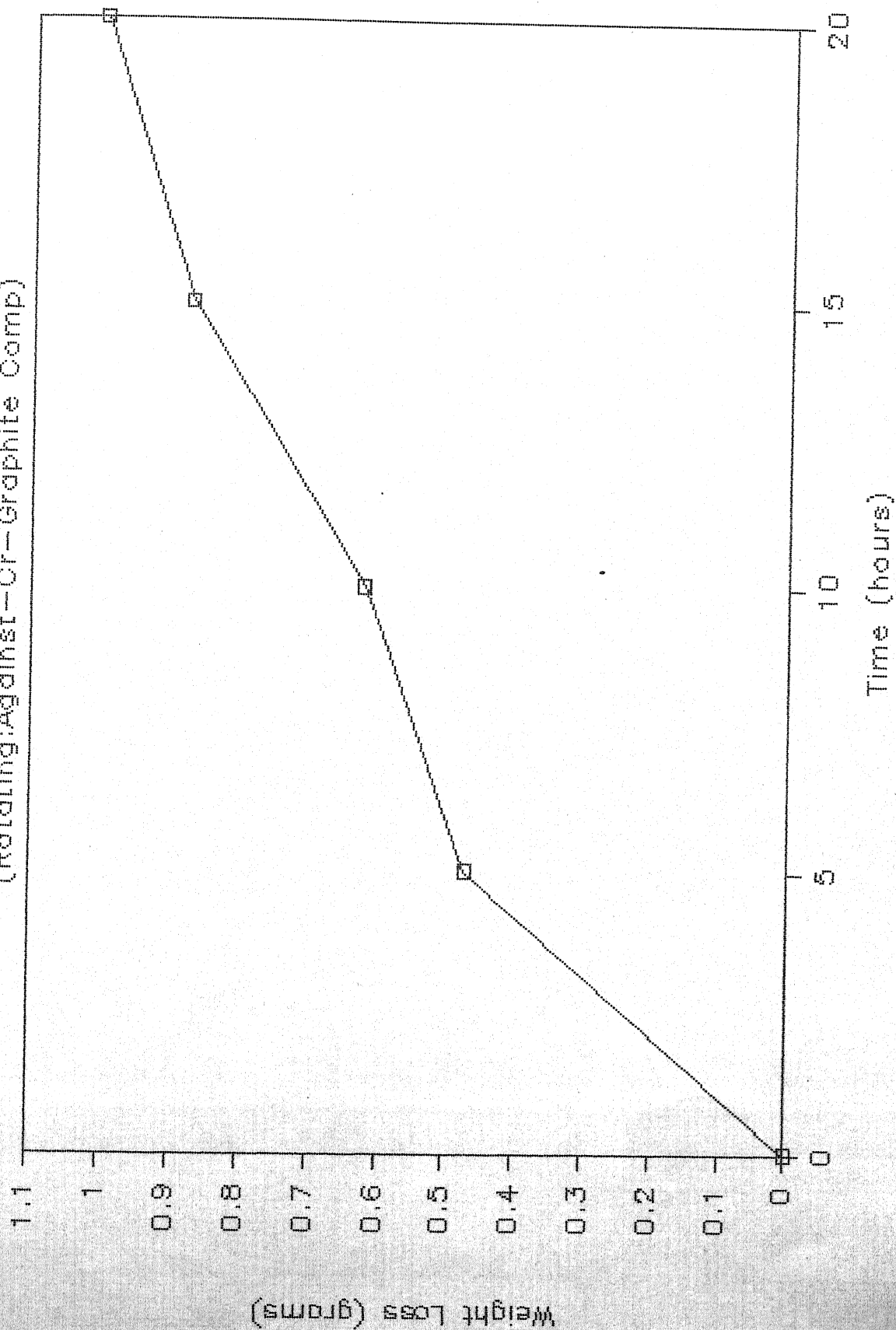


# WEIGHT LOSS VS TIME (Load—100 kg) (Static:Cr—Graphite Comp)



11-DSA

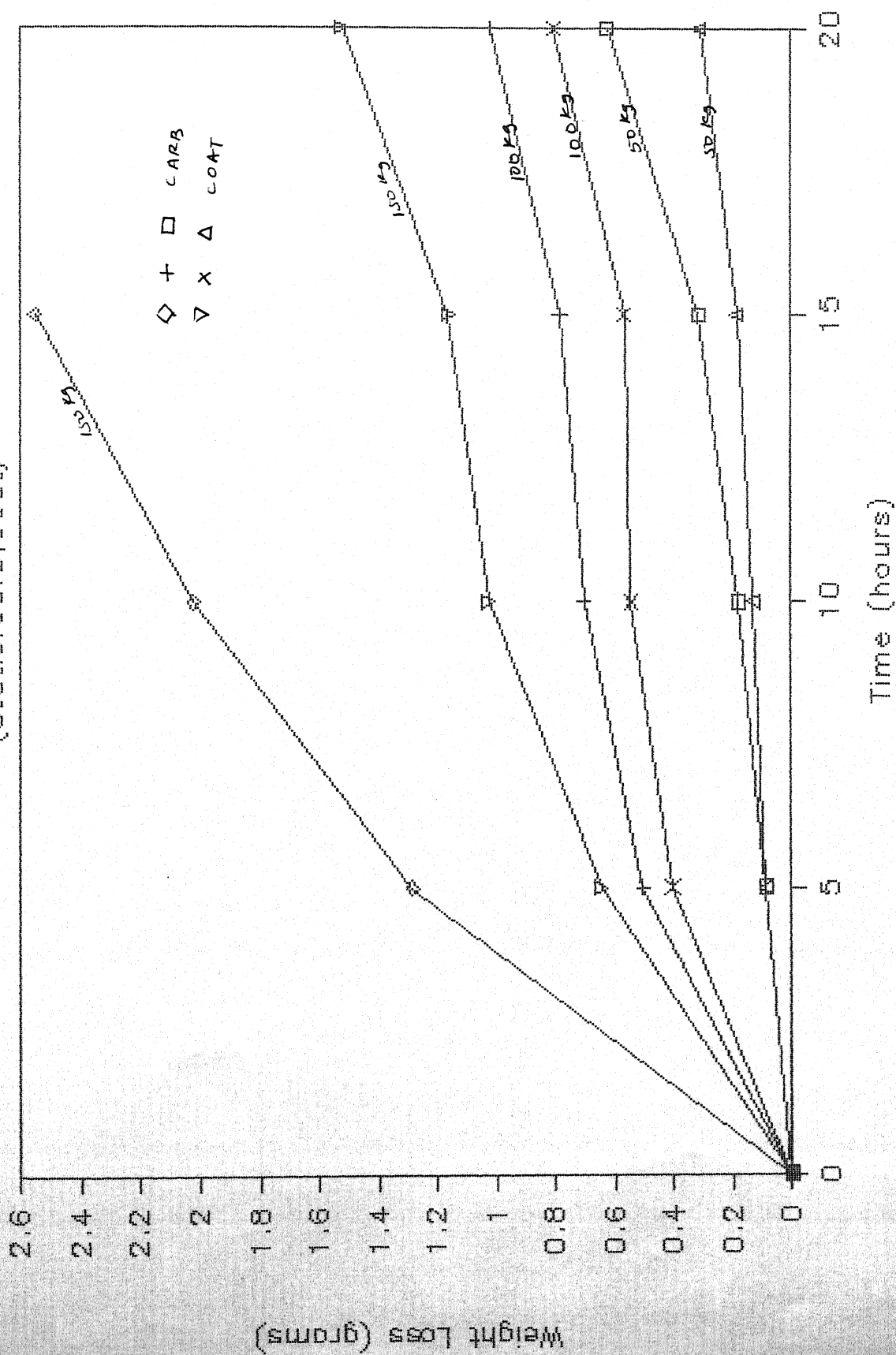
# WEIGHT LOSS VS TIME (Load—100 kg) (Rotating:Against—Cr—Graphite Comp)



12. D5B

# WEIGHT LOSS V\ S TIME

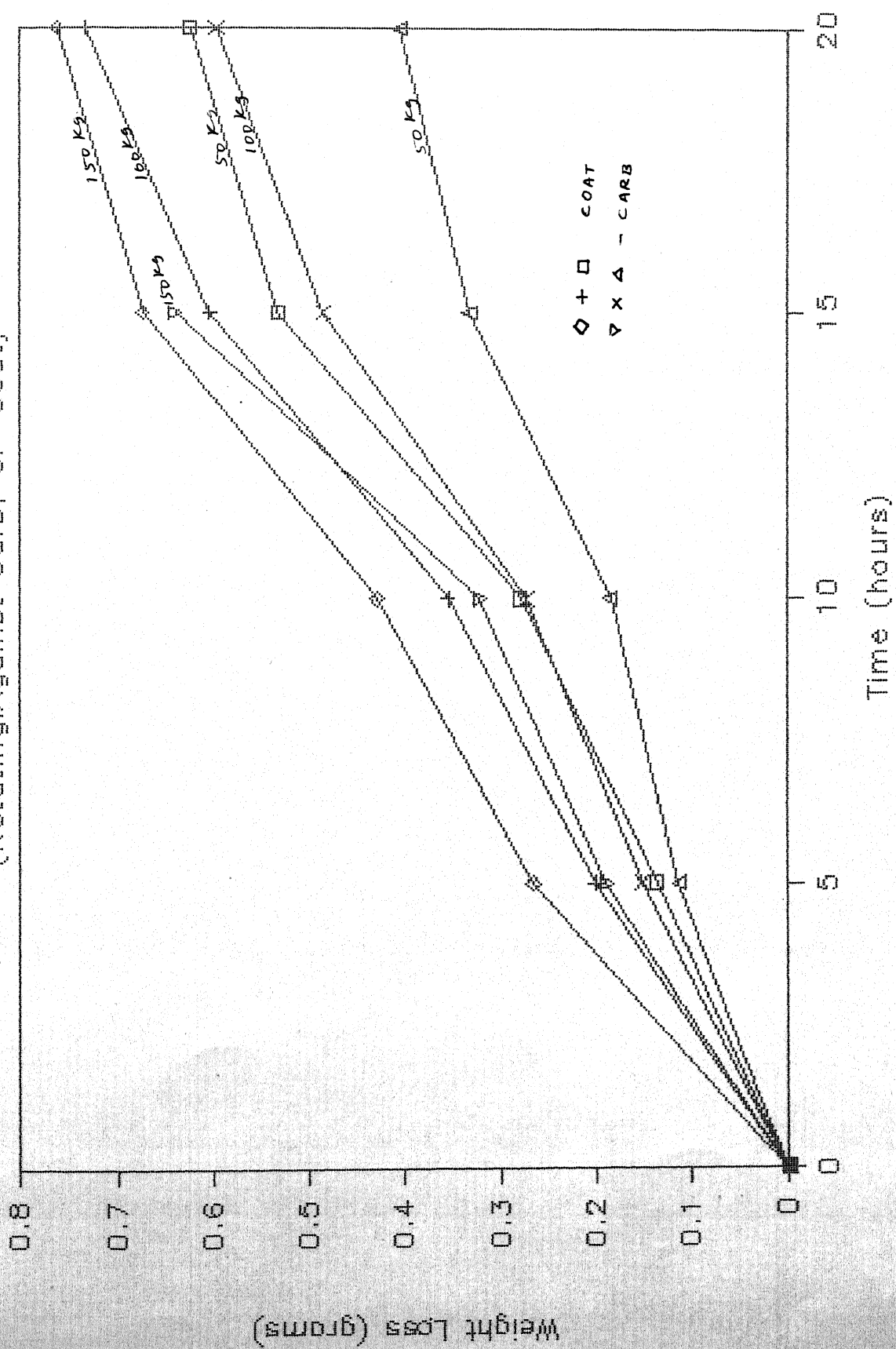
(Static:Carb:Coat)



13-D3A

# WEIGHT LOSS VS TIME

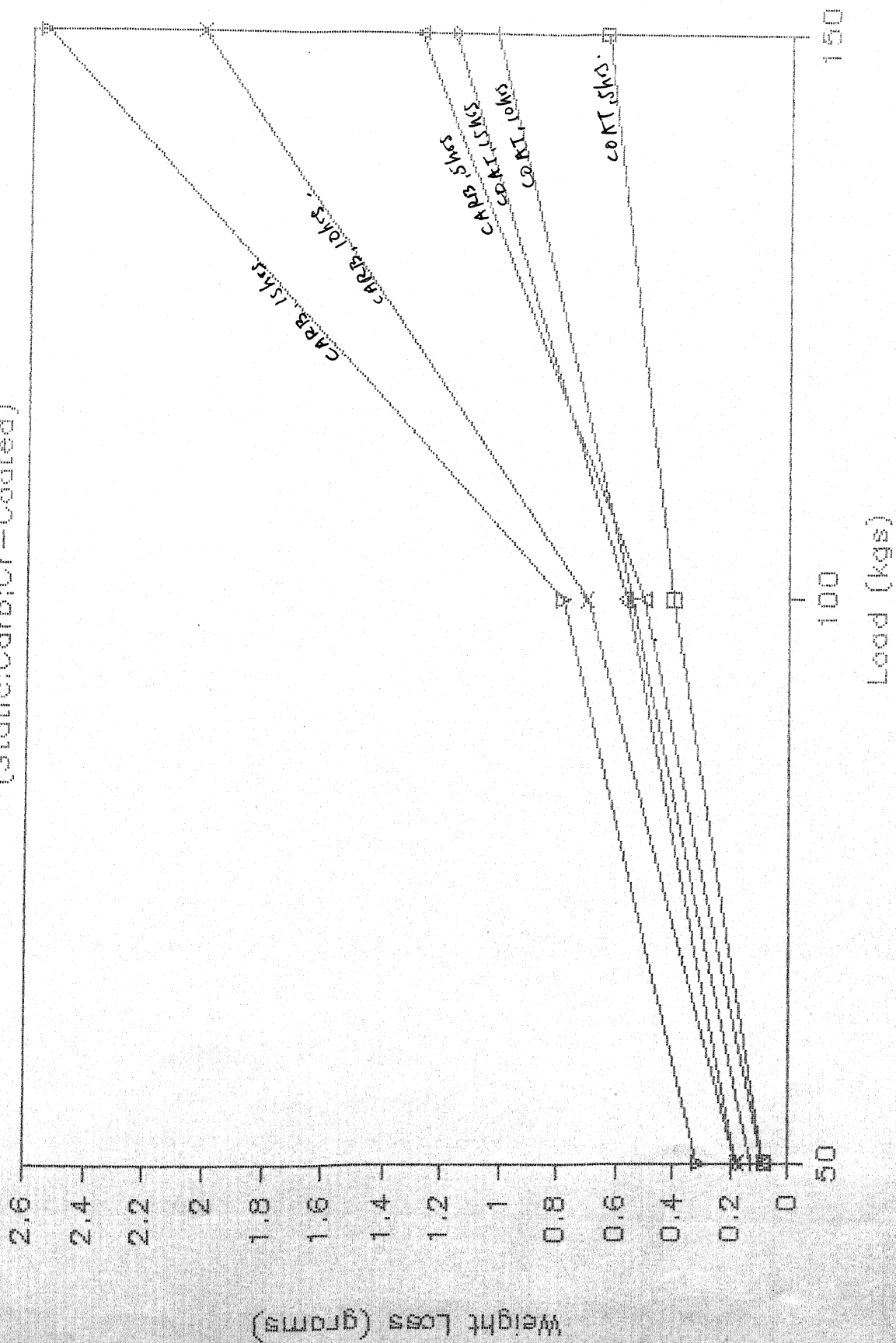
(Rotating Against Carb; Or-Coat)



14.D3B

# WEIGHT LOSS VS LOAD

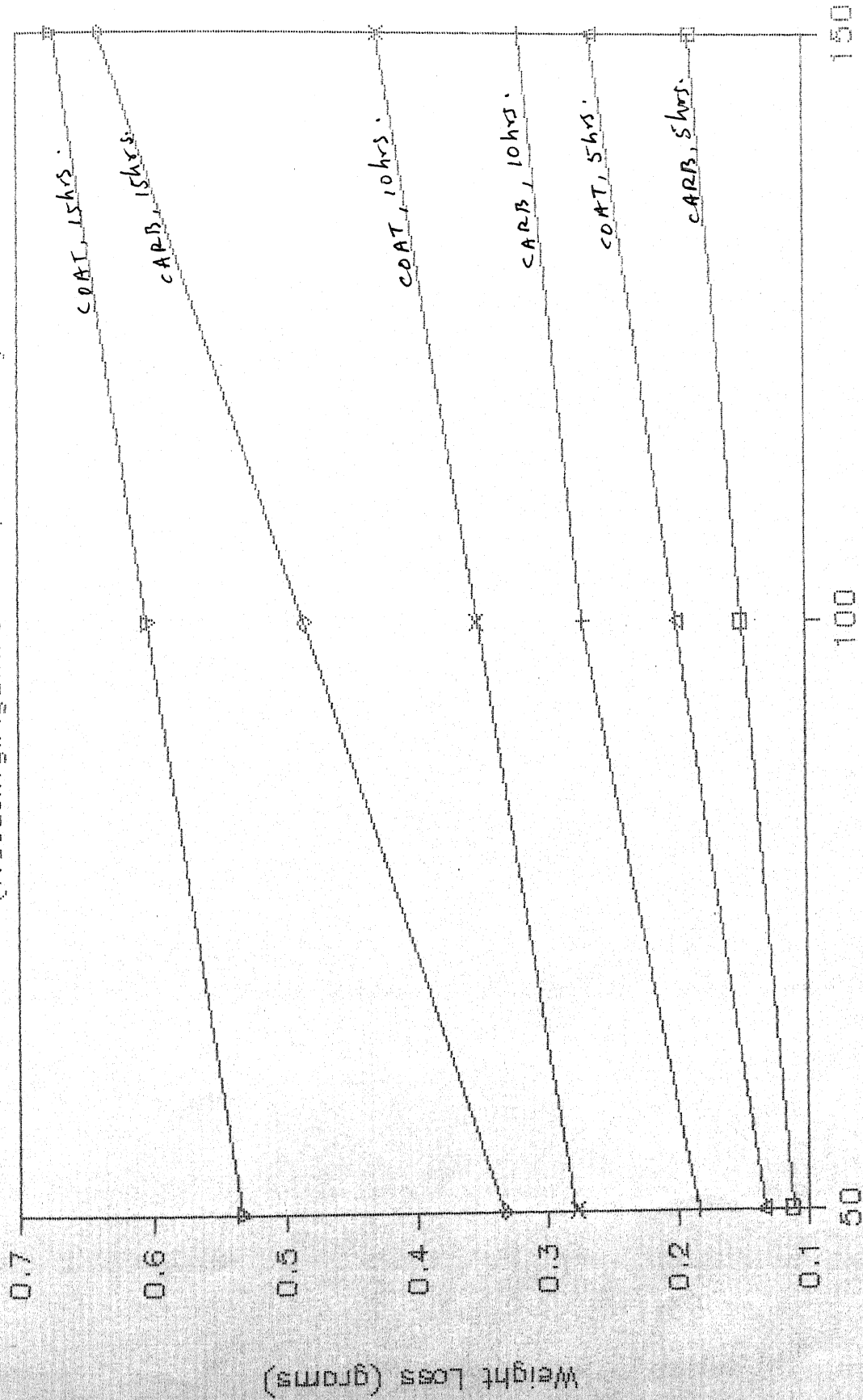
(Static: Carb; Cr-Coated)



15. DL3A.

# WEIGHT LOSS VS LOAD

(Rotating Against Carb; Cr-Coat)

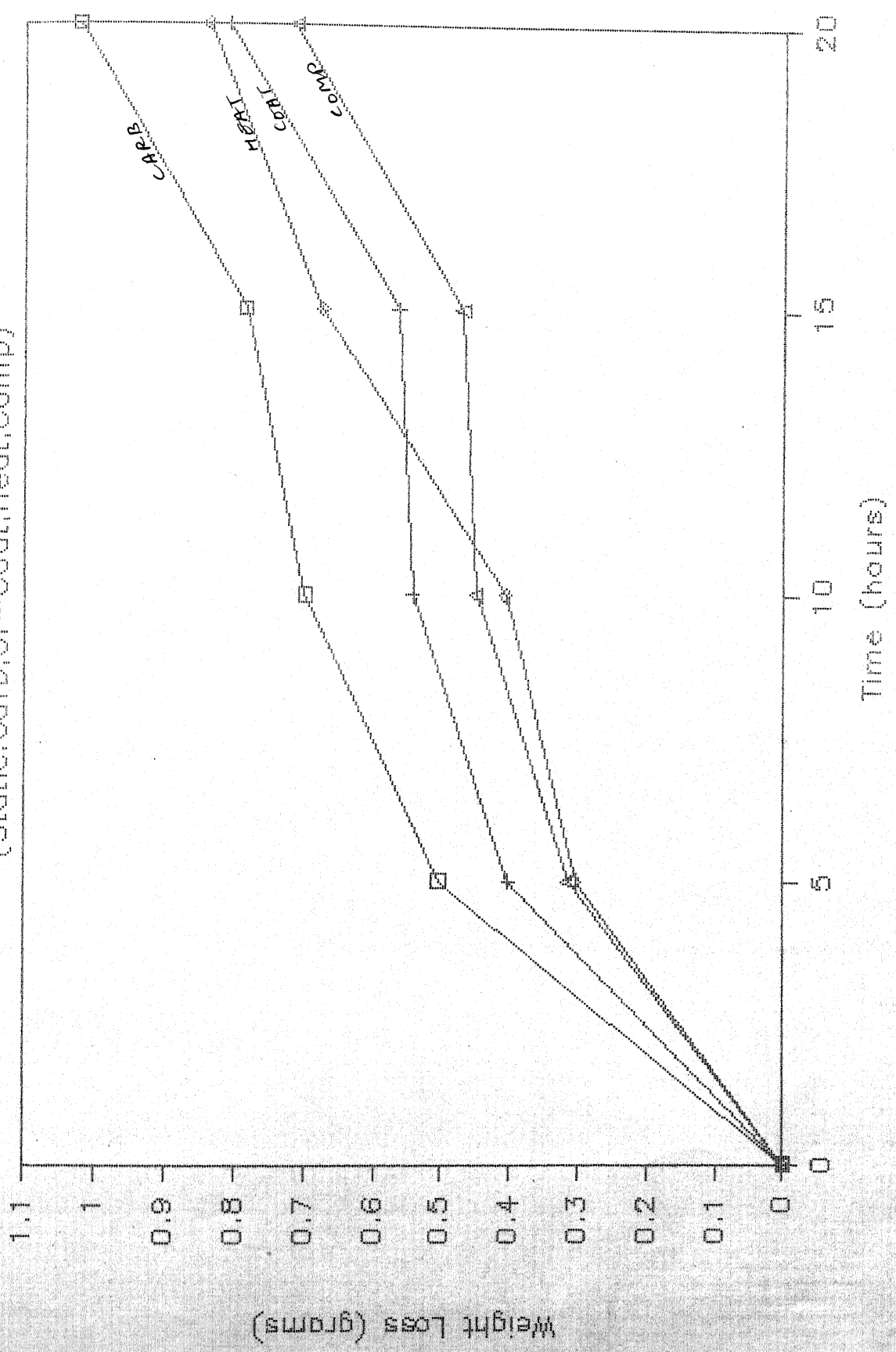


Load (kgs)

16.DL3B

# WEIGHT LOSS VS TIME (Load-100 kg)

(Static; Carb; Cr-Coat; Heat; Comp)



17. D6A



# WEIGHT LOSS VS TIME (Load-100 kg)

(Rotating: Against - Carb, Coat, Heat, Comp)

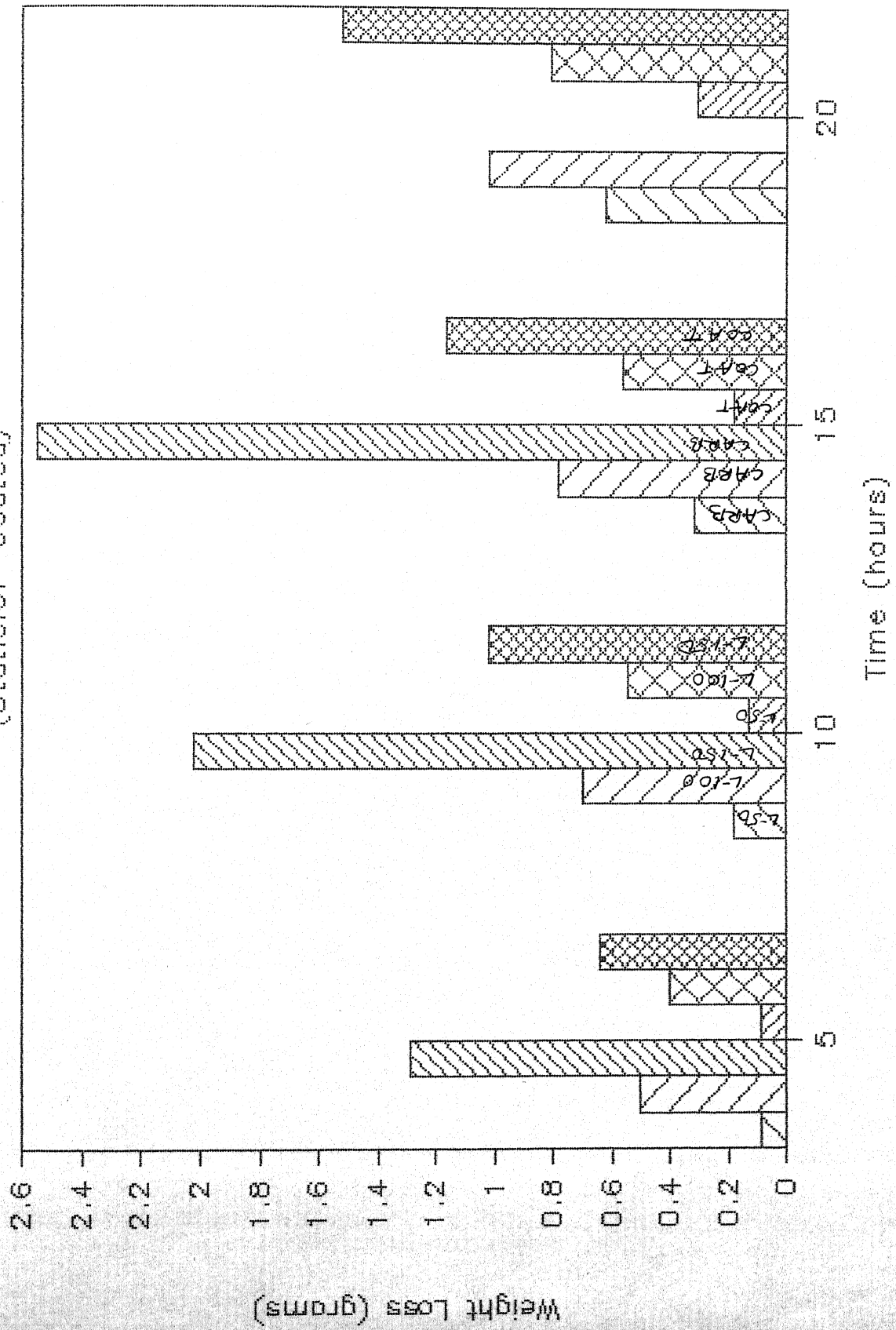


18-D6B



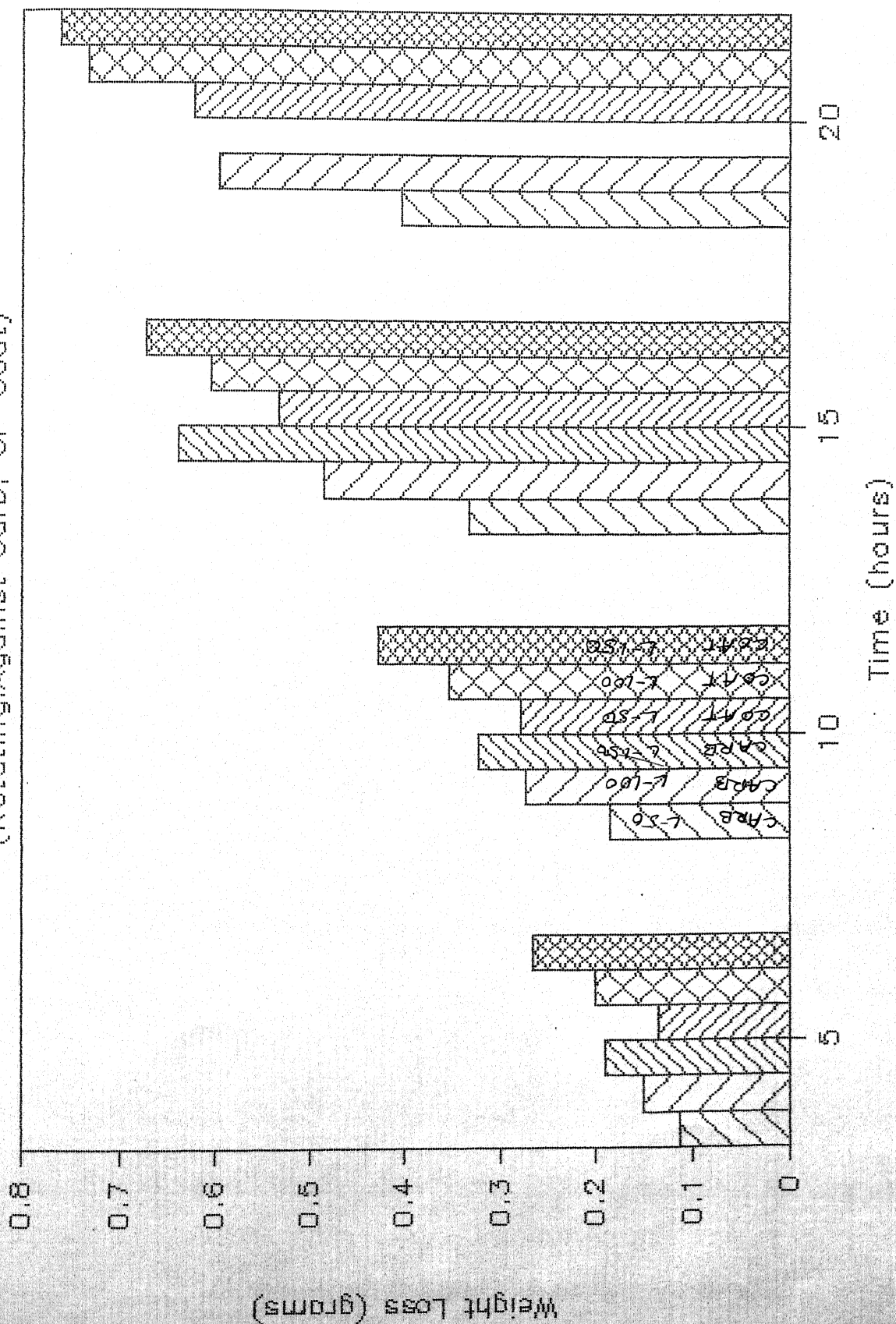
# WEIGHT LOSS V\ S TIME

(Static:Cr-Coated)



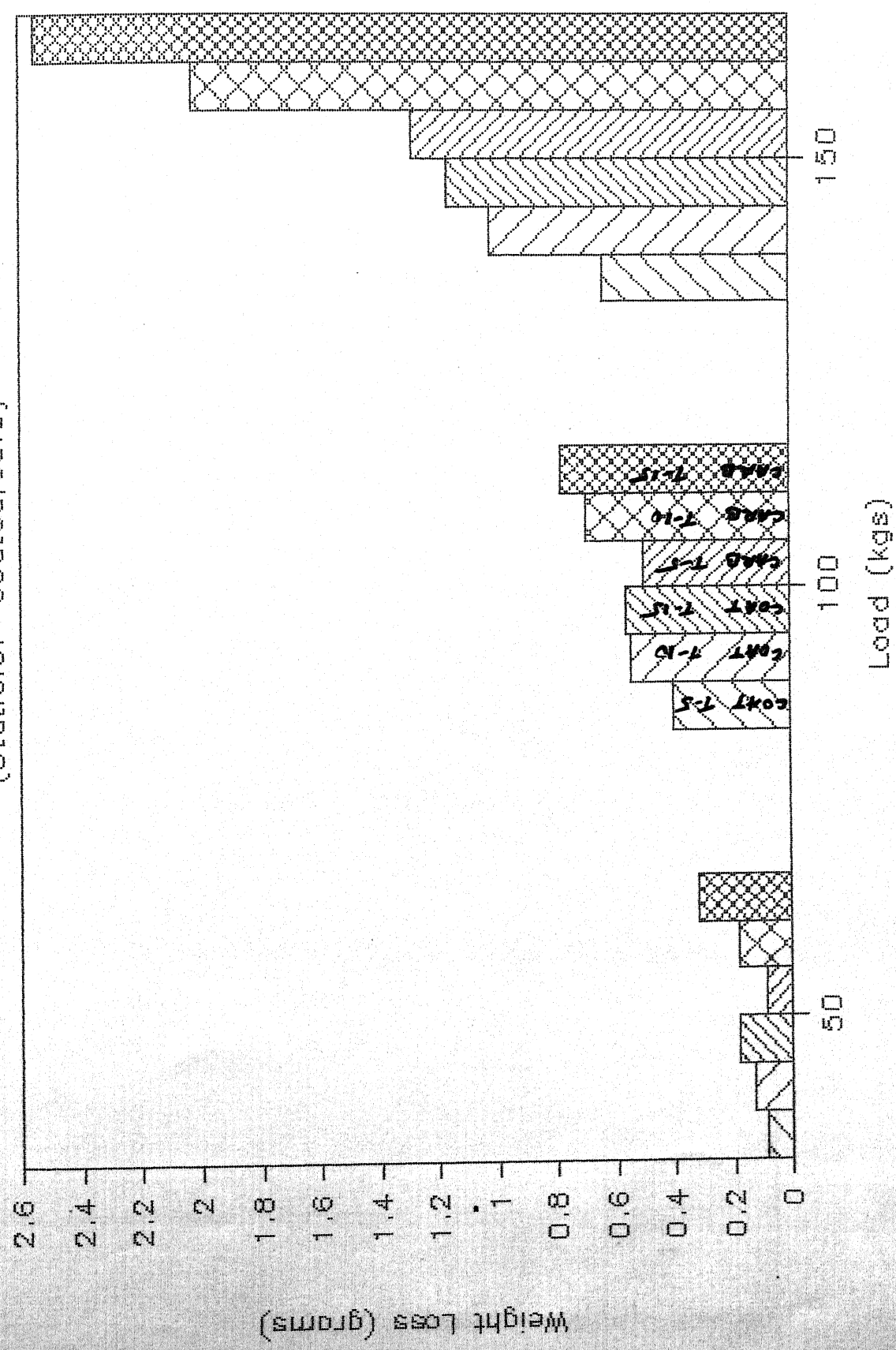
# WEIGHT LOSS VS TIME

(Rotating:Against Carb; Or-Coat)



# WEIGHT LOSS VS LOAD

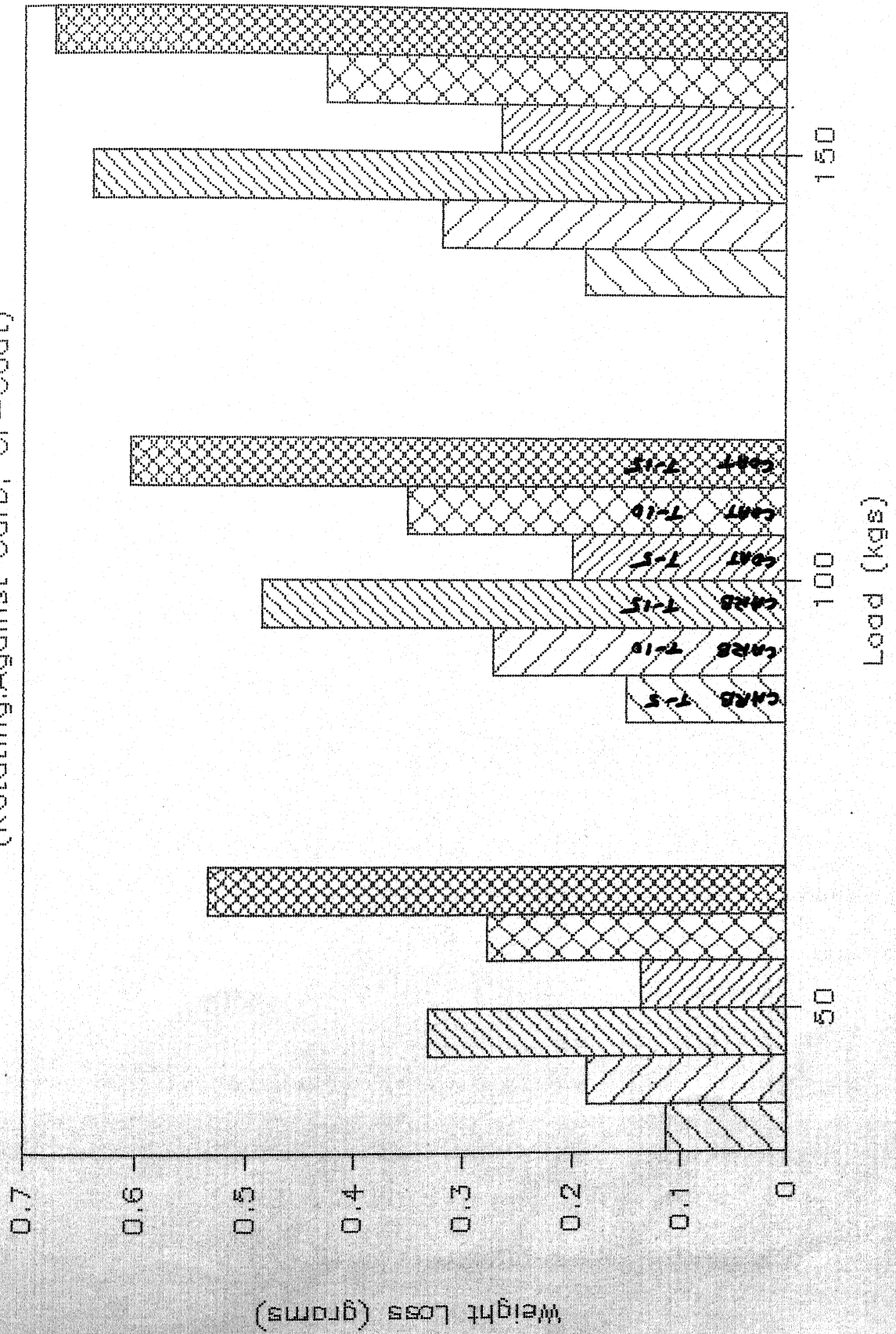
(Static:Or-Coated:Carb)



21.63

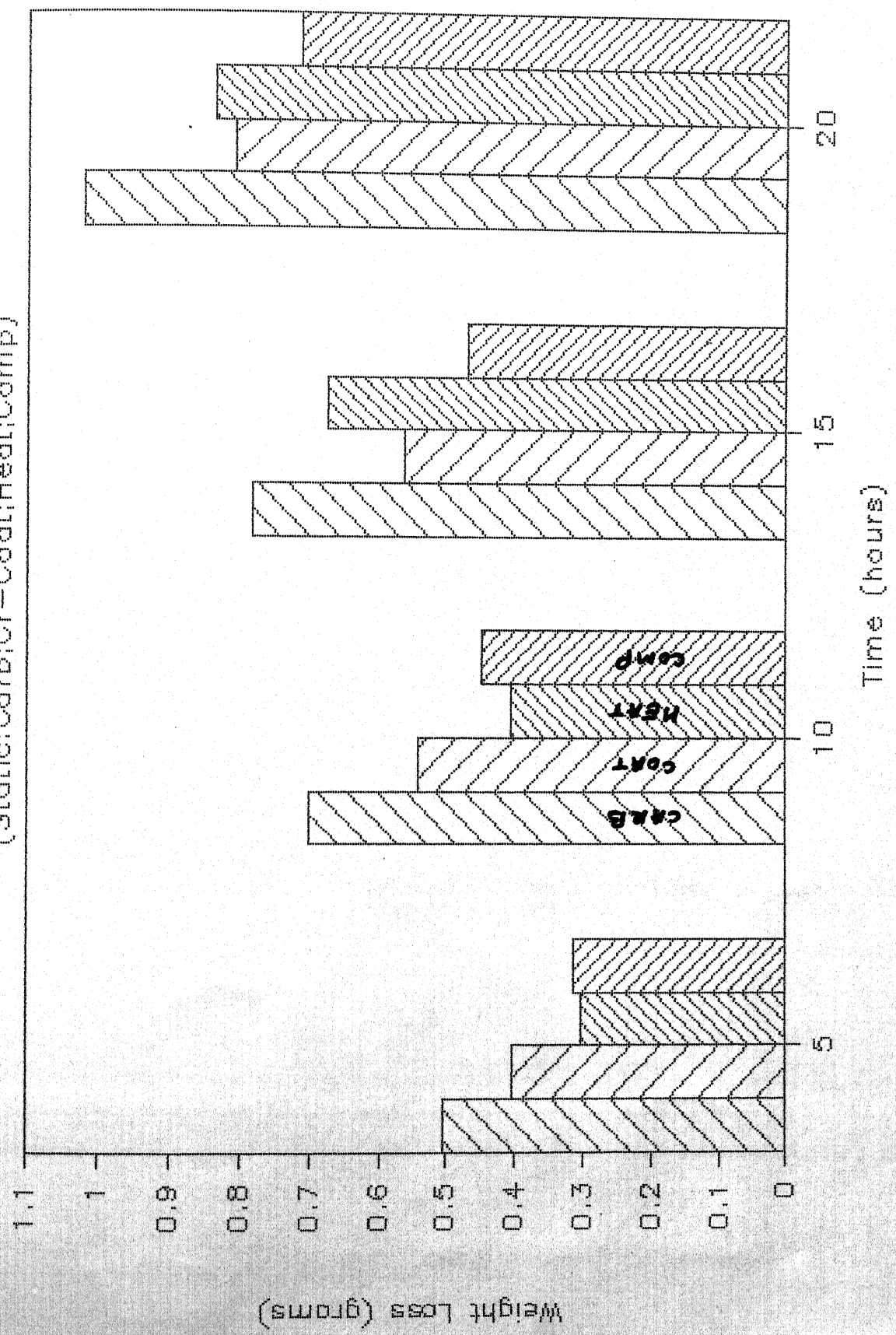
# WEIGHT LOSS VS LOAD

(Rotating:Against Carb; Cr-Coat)



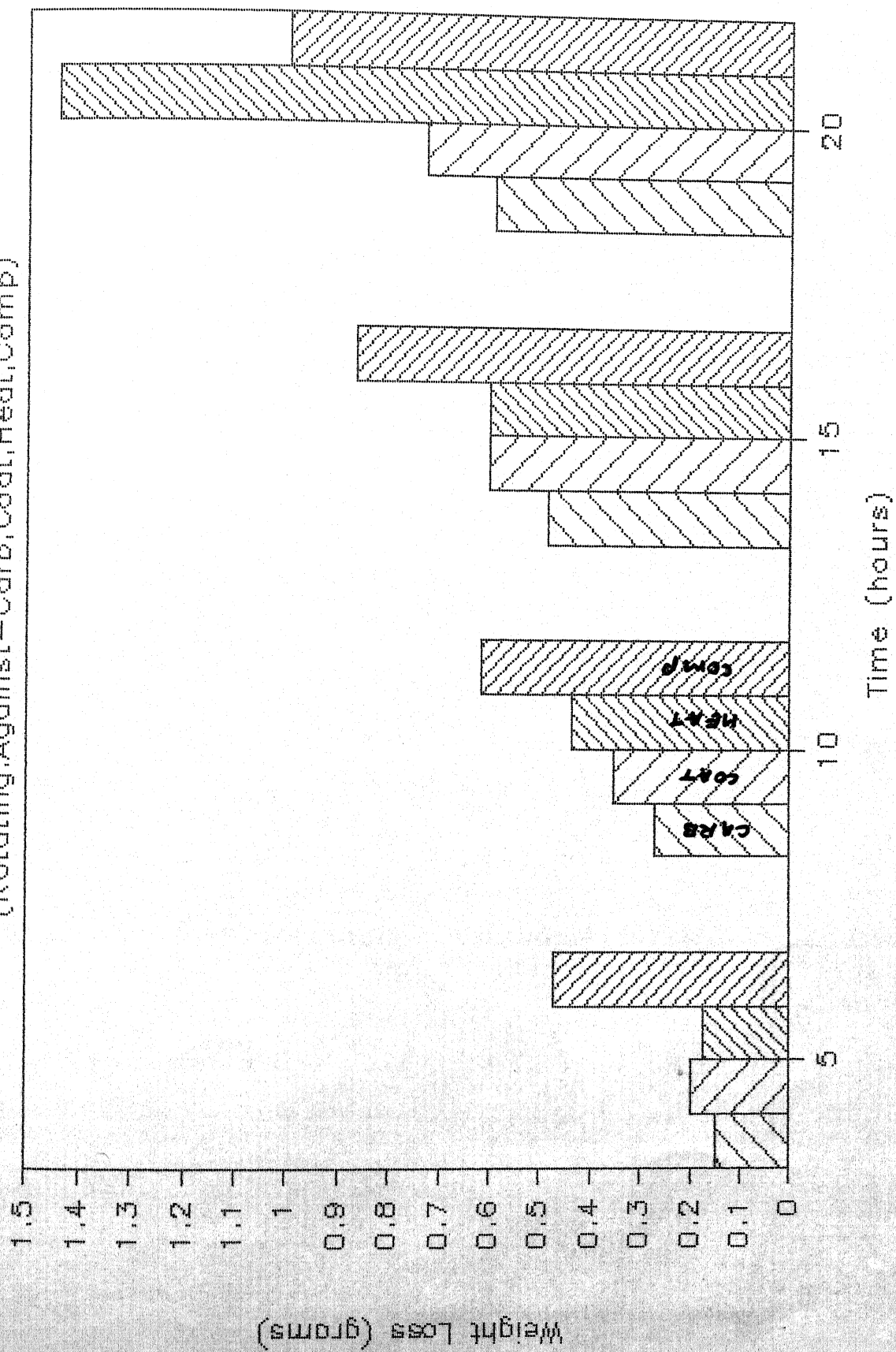
# WEIGHT LOSS VS TIME (Load-100 kg)

(Static:Carb;Cr-Coat;Heat;Comp)





# WEIGHT LOSS VS TIME (Load-100 kg) (Rotating:Against-Carb,Coat,Heat,Comp)



The subsurface voids elongate by further plastic deformation and usually they are directed along the shear deformation lines as can be observed in plates no. 0014 & 0015. These enlarged voids will then coalesce to form longer cracks fairly parallel to the deformation direction, i.e. parallel to the sliding direction.

#### **b) WEAR SHEET FORMATION:**

As deformation proceeds, the subsurface cracks advance to the free surface. The wear sheets were detached from the surface only in selected areas with a perpendicular crack of various length as it is evident from plate no 0013, 0014, 0015. Further sliding will advance the crack to the surface on all portion of the crack front (opposite to the sliding direction). Plate 0015 clearly shows this behaviour for carburized and tempered 100% martensitic steel. This micrograph indicate that the wear sheets have been lifted slightly from the surface since the cracks have just reached the surface. The wear sheet will lift further from the plane of the surface due to the residual stress and strain in the sheet or due to the repeated loading.

The maximum bending is at the left end of the sheet, where it is still in contact with the worn surface, crack will develop at this position. Here ductility plays a major role in wear sheet detachment, since the crack formation by the bending action of the sheet will be enhanced in less ductile metals.

When the wear sheets become detached from the surface, shallow craters are produced from the surface, as shown by plate no. 0017 and 0018. These photographs are for medium carbon steel having 100% tempered martensite.

Plates no. 15 to 16 are for static component in our experiment made of bush material which is carburized and then tempered for 100% martensite low carbon steel.

Plate 17 & 18 are for rotating component which is made of sprocket material i.e. medium carbon steel quenched and then tempered for 100% martensite.

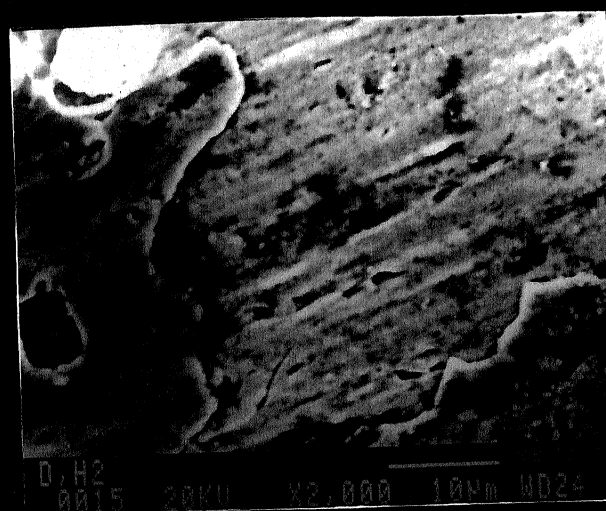
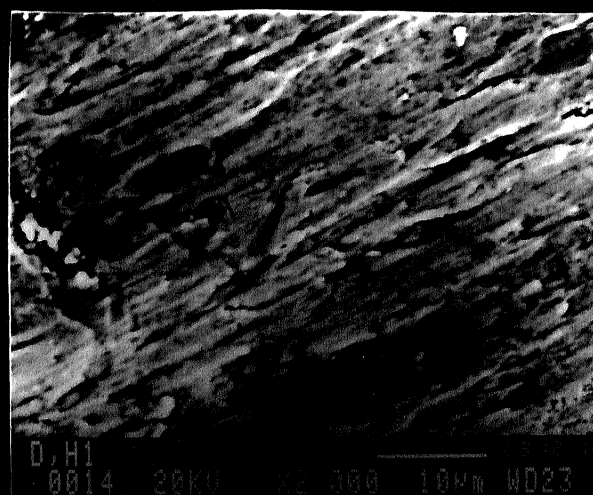
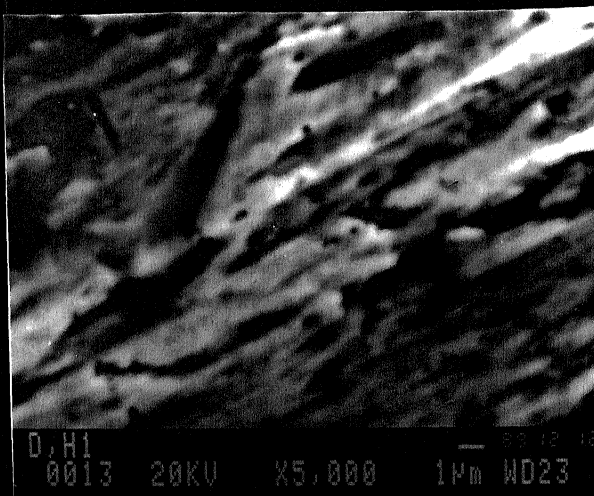
There is clear difference of wear pattern for two components as it is evident from the photographs.

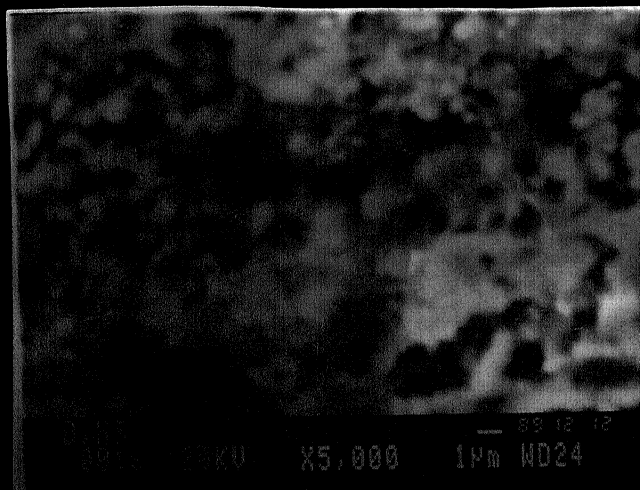
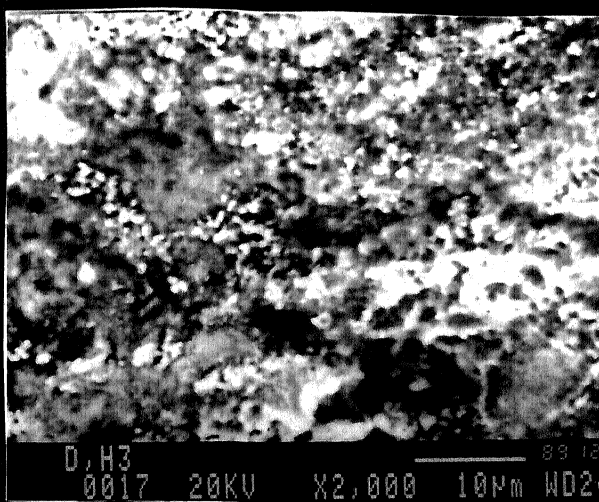
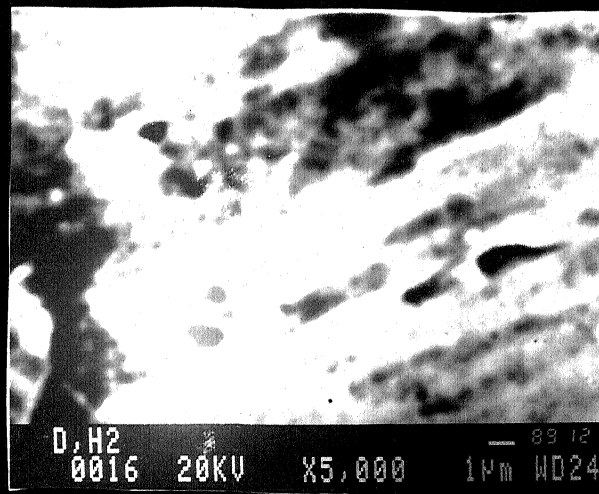
For static component, since it is carburized and then tempered for 100% martensite, because of difference in c/a ratio subsurface void nucleation, crack propagation and chipping would be easier in earlier cases. But for rotating component there is cyclic loading and so due to fatigue, strain hardening takes place and thus chip size would be smaller as it is evident from the plates.

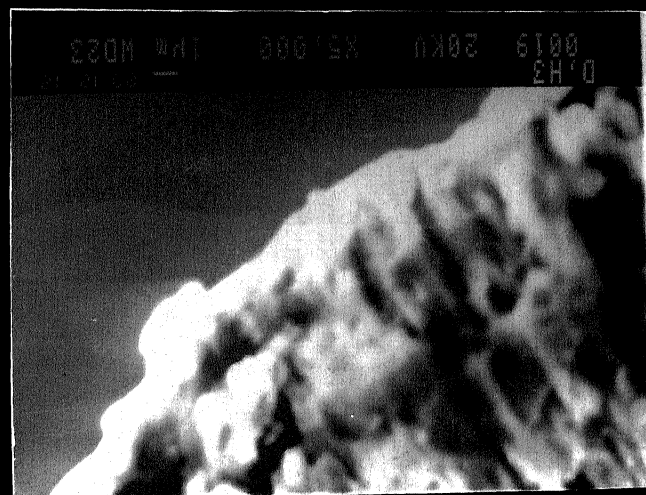
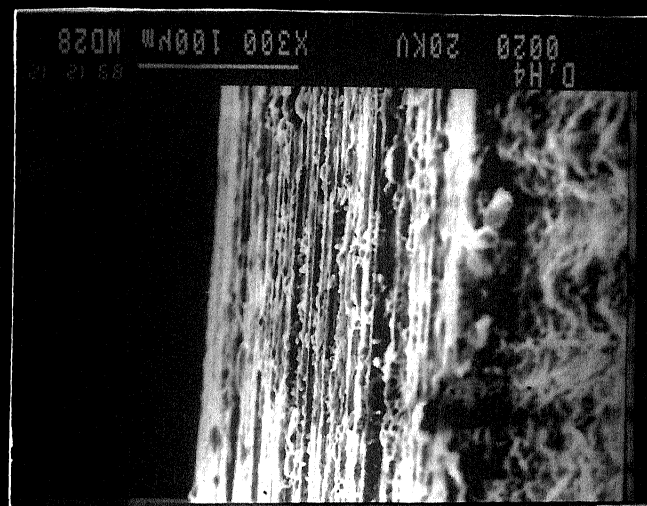
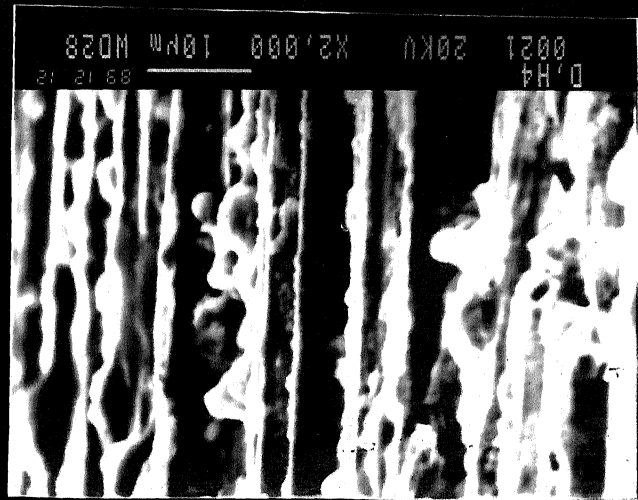
**PLATE 19:** It is a cross-section with Cr-coating on bush material which is static in our experiment. It shows that a considerable thickness of coating took place.

**PLATE 20 & 21:** These are two photographs showing the cross-section of Cr-graphite composite coating which is performed on bush material. There are alternate layers of Cr and graphite distributed evenly all over the coating. Coatings here developed is of considerable thickness.









## CHAPTER 5:

### CONCLUSIONS:

1. In spite of greater surface hardness, carburised-heat-treated steels wears faster than hardened medium carbon steel.
2. From the wear point of view, it is beneficial to use same materials for bush and sprocket with similar heat-treatments (quench hardening and tempering).
3. Chromium coatings on carburised heat treated bush material improves its wear resistance. However it adversely affects the wear rate of sprocket material.
4. Chromium-graphite coatings on carburised heat treated bush material improved its wear resistance more than that by chromium coatings. Overall performance of these coatings is better than any other system.
5. Adhesion theory of wear controls the wear mechanism only in the initial stages and most of the sliding wear process can be explained only on the basis of delamination theory.

## CHAPTER 6

### SCOPE OF FURTHER STUDIES:

1. Due to lack of time and limited scope of my thesis hard particle dispersed coating could not be performed which can be studied to see the result.
2. Here only Cr and Cr-graphite composite coating is performed and studied. But there are many other metals like Ni, W, Al Ag and metal oxides like  $Al_2O_3$ ,  $TiO_2$ ,  $Cr_2O_3$ ,  $MgO$ ,  $SiC$  etc of which coating can be performed and on the basis of results they can be compared.
3. We had studied only about improving the life of bush material, even at sometimes at the cost of sprocket material and on that basis I am reaching at certain conclusion. But relative economic viability of various processes are also to be studied which can have tremendous practical importance.
4. There are many other sophisticated surface treatment like carbo-nitriding, laser treatment, plasma spraying which can open a bounty of new avenues and we may come up with fascinating new results, which can also be studied in great detail.

## CHAPTER-7

### REFERENCES

1. Nwoko, V.D., Shreir, L.L.J. Applied Electrochem 3/2/ 137-42 (1973)
2. Greco, V.F.; Baldauf, W. "Plating. Mar. 250 7 (1976)
3. Kedward, F.C. et al. Trans Inst. Metal Finish 54 8-16 (1976)
4. Kedward, F.C.; Metallurgica, 7916 225-8 (1969).
5. Brandes, E.A.; Goldthrope, D. Metallurgica, Nov 195-8 (1967)
6. Young, J.P. N.B. SIR - 74-115 (1979)
7. Skominas, V et al Liet TSR Mokslu Akad Darb Ser B(1) 101-6 1971
8. Addison, C.A.; Kedward, E.C. Trans. Inst. Metal Finish 55(Pt 2) 41-6 (1977).
9. Kedward, E.C. et al Tribol Inst 7(5) 221-7(1974)
10. Young, J.P. NB SIR -74 -615 (1974)
11. Wagner, L.H.; Edickson, R.P. NTIS, ad.no 74 7767- (1972)
12. Kedward, E.C., et al Brit 1, 220, 331 (1971)
13. Vest, C.E. Bazzarre, D.F. Metal Finish 65 (11) 52 - 8(1972)
14. Kedward, E.C. Lesson, J. Brit 1, 236, 954 (1971)
15. Borodin, J.N. Elektron Obrab. Marter. May 22-4 (1971)
16. Dushevski J.V. Borodin J.N. Izv. Vyssh. Ucheb Zavel, Khim Teknof 15(9) 1091-4 (1972)
17. Borodin J.N. et al. Zashch. Met 13(2) 233-5 (1972)
18. Zentsova, E.P. et al. Zashch. Met 13(2) 233-5 (1977)
19. Saifullin R.S. et al Bi kl Elektokhim 1-2, 50-4 (1973)
20. Loeffler d. Gerr. offen 2, 112, 684 (1972)
21. Kedward, E.C. et al Brit 1, 265, 472(1972)



22. Loeffler, D. Galvantechnik, 65(5) 360-3 (1974)
23. Tomaszewski, T.W. et al. Plating. Nov. 1234-9 (1969)
24. Bazzard, R. Boden, P.J. Trans Inst. Metal Finish. 50(5)  
207-10 (1972)
25. Ep;K, A.P. et al, Zashch; Pokrytiya Met. 8,91-3 (1974)
26. Samsonov. G.V. et al Porosk metal 1987,1, 7-10 (1977)
27. Fedor Chenko, I.M. et al. Porshk, Metal (3) 56-9 (1975)
28. Guslienko, Yu A. Mater. Izdeliya, Poluchanye Metodam. Poroshk,  
Metal 164-9 (1974)
29. Kedward. E.C. Brit. 1,220, 332 (1971)
30. Martin, P.W. Metal Finish. J. 11(1130) 399-403 (1965)
31. Foster, J. ;Kariapper, A.M.J. Trans.Inst.Metal Finish  
50(pt5) 207-10 (1972)
32. Guglielmi, N.J. Electrochem. Soc. 119(8) 1009-12 (1972)
33. Nam P.Suh, Wear, 44(1977) 1-16
34. Nam P.Suh. Wear, 25(1977) 111-124
35. J.R. Flaming and N.P. Suh, Wear 44 (1977) 39-56
36. J.R. Flaming and N.P. Suh, Wear 44(1977) 57-64
37. Jarlen Don and D.A. Rigney, Wear 105 (1985) 63-72
38. S. Jahanmir and N.P. Suh, Wear 44(1977) 87-99
39. N.P. Suh, N. Saka and S. JAHANMIR, WEAR 44 (1977) 127-134
40. S. Jahanmir, Wear, 103 (1985) 233-252
41. J.J. Pamies- Teixeira, N. Saka and N.P. Sah, Wear  
44(1975) 65-75
42. F.H. Stott and G.C. Wood, Tribol. Out., 11-(1978) 211-218
43. S. Jahanmir and N.P. Suh, Wear 44(1977) 17-38.
44. Konzina, G.V. Tr. Kishinev, Sel'Skekhoz. Inst. 59, 22-4 (1970)